

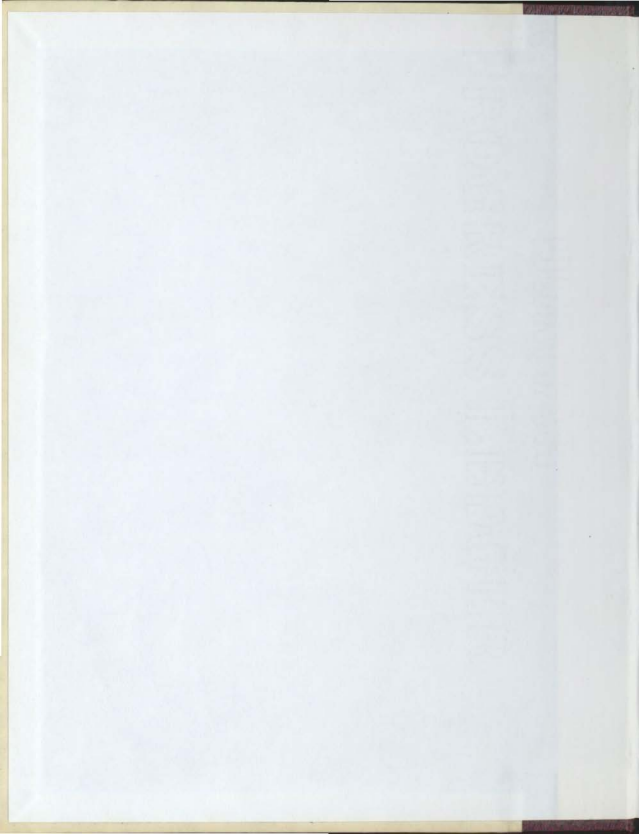
THE ADSORPTION OF TETRACHLOROETHYLENE  
AND TRICHLOROFLUOROMETHANE  
ON ANHYDROUS NICKEL SULFATE

CENTRE FOR NEWFOUNDLAND STUDIES

**TOTAL OF 10 PAGES ONLY  
MAY BE XEROXED**

*(Without Author's Permission)*

GEORGE A. KINLOCH, B. Sc.







THE ADSORPTION OF TETRACHLOROETHYLENE AND  
TRICHLOROFLUOROMETHANE ON ANHYDROUS NICKEL SULFATE

A Thesis

by

Ⓢ George A. Kinloch B.Sc., r.m.c.

Submitted in partial fulfillment  
of the requirements for the degree of  
Master of Science

June, 1969

Memorial University of  
Newfoundland

ACKNOWLEDGEMENTS

The author wishes to express his sincere appreciation to Dr. W. D. Machin for his supervision and encouragement during this investigation. Thanks are also due Mr. M. B. Bajpai for many helpful discussions and suggestions and Mr. Paul Gillard for his assistance with the calculations.

The author wishes to express his appreciation to the Technical Services personnel who assisted with the design and construction of the apparatus.

Finally the author wishes to thank Miss R. Barron who typed this thesis.

CONTENTS

	page
Acknowledgements	2
Abstract	6
Introduction	7
Experimental	12
1. Adsorption Techniques	12
2. Construction of the Apparatus	14
a. The Balance and Case	14
b. Light Sources and Light Sensing Devices.	15
c. Measurement of Weight Change.	15
d. Pressure Measurement.	16
e. Thermostated Bath.	17
3. Calibration of the Balance.	17
4. Vacuum Line	24
5. Materials.	25
6. Experimental Procedure.	28
Experimental Results	30

	page
Discussion.	30
1. The Isotherms.	30
2. Surface Area and Monolayer Capacity.	37
a. Monolayer Capacity.	37
b. Surface Area.	38
3. Heats of Adsorption.	40
4. Entropies of Adsorption.	42
a. Experimental Entropy Changes.	42
b. Theoretical Entropy of Condensation.	44
c. Theoretical Entropy of Two Dimensional Gas.	46
5. Capillary Condensation.	49
Summary.	63
Literature Cited.	66
Addendum I.	137
Examiners, Remarks and Replies to these remarks.	

	page
Appendix 1. Calibration of the Spoon Gauge	70
2. Balance Calibration.	79
3. Graph of log vapour pressure vs $\frac{1}{T}$	85
4. Tabulation of Sorption Data.	86
5. BET Plots.	106
6. Isosteric and Differential Heats of Adsorption.	110
7. Standard Entropies and Heat Capacities of Adsorbates.	118
8. Theoretical Entropy Change for Transition from Gas to Liquid for Tetrachloroethylene and Trichloro- fluoromethane.	119
9. Experimental Entropy Changes Accom- panying Adsorption and Desorption Experimental Entropy of Adsorbed State	121
10. Theoretical Entropy Change for Transition from Three Dimensional to Two Dimensional Gas for Tetrachloroethylene and Trichlorofluoromethane.	131
11. Table of $\theta$ and $\frac{-1}{\log \frac{P}{P^0}}$ for inverse Kelvin Equation Plots.	132

ABSTRACT

Tetrachloroethylene and trichloro-fluoromethane exhibit hysteresis when adsorbed on anhydrous nickel sulfate. Analysis of the heats of adsorption and the entropies of the adsorbed substances suggests that condensation occurs during adsorption. This is corroborated by analysis of the data with the Kelvin equation. This analysis also indicates that the angle of contact between the condensed adsorbate and the adsorbent is not zero as is usually assumed, but is in fact, finite. The data suggest that layers of adsorbate of only two molecules' thickness can exhibit liquidlike properties. The shape of the isotherm suggests that the adsorbent consists of parallel plates separated by capillary spaces within which condensation occurs. The plates may move apart as adsorption progresses to accommodate large volumes of adsorbate between the plates.

## INTRODUCTION

Sorption isotherms usually fall into one of the classifications proposed by Brunauer, Demming, Demming and Teller (1,2). Of these, Types II and IV commonly exhibit hysteresis; that is, the quantity sorbed during desorption does not retrace the path followed during adsorption.

Zsigmondy (3) postulated that hysteresis was caused by capillary condensation associated with impurities on the surface. This postulate is, however, inconsistent with the existence of persistent, reproducible hysteresis. A more general theory was developed by Kraemer(4) and McBain (5) which attributed hysteresis to condensation in capillary spaces with constricted channels of communication. During adsorption cylindrical menisci form on the surfaces of the capillaries which eventually block the pore entrance and form spherical menisci. Desorption takes place from these spherical menisci over which the vapour pressure differs from that over the cylindrical menisci, thus accounting for the hysteresis. The capillary spaces associated with this may be cylindrical, slit shaped (6), or in the form of parallel plates (7,8). If no constrictions are involved in the capillary system, the vapour pressure must reach saturation level for the adsorbate, or the layers of adsorbate must completely fill the pore space before the spherical meniscus may be formed.

When capillary condensation occurs in cylindrical pores, the shape of the hysteresis loop may be related to the structure of the pore system (9,10) by the Kelvin equation:

$$\ln \frac{P}{P^0} = - \frac{2 \gamma V \cos \phi}{RT \cdot r} \quad \dots (1)$$

where;

$p$  = vapour pressure of liquid over the meniscus.

$p^0$  = vapour pressure of the bulk liquid.

$\gamma$  = surface tension of the liquid.

$V$  = molar volume of the liquid.

$\phi$  = contact angle.

$R$  = the gas constant.

$T$  = the temperature.

$r$  = the radius of the pore.

de Boer (9) distinguished five types of hysteresis loops according to the slopes of the adsorption and desorption branches of the isotherm and the relative pressures at which the closure points occur. These types are shown in Figure 1. The Type A loop is associated with condensation in tubular capillaries, tubular capillaries with slightly widened parts or ink bottle pores with wide necks not much greater than the width of the bodies. The Type B loop is associated

with ink bottle pores with narrow necks and wide bodies, slit-shaped pores, or condensation between parallel plates. The Type E loop, which is similar to the Type A loop, is associated with pore mouths of uniform size and pore bodies of widely distributed radii.

The upper closure point of the hysteresis loop may be readily associated with pore size, but the lower closure point may have only a limited relevance to pore size (11). This point occurs when the menisci in the smallest pores change from spherical to the cylindrical form. This change may be inhibited if the free volume in the pore is less than the critical bubble size of the adsorbate.

Hysteresis may also be caused by the change of structure of the adsorbed state that occurs during adsorption and persists during desorption until some critical pressure is reached at which the adsorbate reverts to its initial state (11). Hysteresis caused by such changes could be distinguished from capillary effects by examining the conformation of the system to the Kelvin equation.

The state of the adsorbate may be examined in terms of its thermodynamic functions. Young and Crowell (12) have reviewed and discussed the development and applications of thermodynamics to surface phenomena. The heats and entropies of sorption may be compared to the heats of vaporization and the entropies of the adsorbate in the form of various models such as a liquid or two-dimensional gas.

FIGURE - ITypes of Hysteresis Curves.Type AType BType CType DType E

Tetrachloroethylene and trichlorofluoromethane exhibited Type B hysteresis when adsorbed on anhydrous nickel sulphate. The isotherms were similar to those obtained by Barrer and MacLeod (7) with various adsorbents on montmorillonite clays. This similarity suggested that the hysteresis was due to condensation of the adsorbates within a parallel plate structure. The entropies of the adsorbed states were calculated from the experimental data and compared to the entropies of the liquid states and to the entropies calculated for the adsorbates in the two-dimensional gas state. The heats of adsorption were compared to the heats of vaporization of the adsorbates. The behaviour of the adsorbate was examined relative to the Kelvin equation. The evidence suggested that condensation occurred within a parallel plate structure in which the plates may move apart to accommodate the adsorbate. It was also found that the angle of contact between the adsorbate and adsorbent is finite and not zero as is usually assumed.



EXPERIMENTAL1. Adsorption Techniques.

The two primary techniques used in the study of sorption of gases on solids are volumetric and gravimetric. Volumetric methods have been reviewed by Young and Crowell (12) and by Gregg and Singh (13).

Gravimetric methods of studying adsorption have been reviewed by Thomas and Williams (14), Thomas and Thomas (15), Gregg and Singh (13), and by Honig (16).

The simplest device is the quartz spring as developed by McBain (17). The extreme fragility of silica has led others to use metal alloys as a material (18). The utility of springs is limited in that while increasing the thinness of the spring increases the sensitivity, it diminishes the load that can be born by the spring. Springs have been developed which have a sensitivity of 0.01% of the load (19). Further deficiencies of springs are their susceptibility to the effects of vibration, convection currents, and buoyancy.

The cantilever balance uses the deflection of a beam rather than the extension of a helix to measure weight change. The sensitivity of a cantilever is limited in the same manner as with springs; and are also susceptible to errors arising from convection currents and buoyancy effects.

A balance incorporating a symmetrical beam minimizes the effects of buoyancy, convection currents and vibration. The beam is usually made of quartz, a material that is both rigid and relatively inert, and not subject to deformation due to temperature.

Various means have been employed to suspend the beam. Tungsten wires have been used, although they are subject to lateral yaw. Pivots such as sharp point tungsten resting in quartz cups (20) or knife edge pivots (21) have been used. They can bear greater loads than the pin type pivots but are still susceptible to errors arising from deformation of the pivot or its seat and irregularities in the pivot surfaces. Pivots may also be of the meter type (22,23). Such pivots are less susceptible to deformation of the pivot surfaces under load and are not as susceptible to misalignment of the pivot surfaces as are the others, but are liable to errors arising from irregularities in the pivot surfaces as well as to errors arising from the greater friction between these surfaces.

The beam position may be determined with a telescope, electronically, or by photo-electric means. The weight change may be measured in terms of the beam deflection. This is a simple procedure, but limits the range of the balance, and tends to maximize errors arising from irregularities in the pivot surfaces, effects of deformation, and assymetry in the balance. The balance may be used as a null instrument in which the

change in weight is measured as a function of the force needed to restore the balance to a reference position. This force is usually provided by a solenoid incorporated in the balance. Used as a null instrument, errors due to deformation of the balance, irregularities in the pivot surfaces, and assymetry of the beam are minimized. In addition, the solenoid serves to damp the balance vibration and oscillation, and may be conveniently used with a recording instrument. Thermal drift in the electronic components is easily eliminated by thermostating them.

Balances having sensitivities of better than  $1 \mu\text{g}$  have been built using all the above means of support and measurement. The meter movement pivot, in which pivot and solenoid are combined in one unit, and electronic weight measurement offer the advantages of ease of construction, robustness and simplicity.

## 2. Construction of the Apparatus.

### a. The Balance and Case.

The balance was similar to that described by other workers (22,23). The beam, shown in Figure 2, was constructed of 1 mm quartz rods and cemented to the coil of a microammeter (General Electric Type 91). The beam assembly was then mounted on a frame of 2 mm quartz rods. The sample and counterweight were suspended from the beam with chains made of short quartz rods. This assembly reduced vibration in the hangdowns (25). Two

aluminum foil vanes were cemented to the beam.

The balance case was made of 40 mm pyrex tubing. "O" ring seals were used to allow access to the case and to connect the legs to the balance case. Leads to the microammeter movement were passed through the top of the balance case and connected to the potentiometer circuit shown in Fig. 5. The overall balance assembly is shown in Fig. 3.

b. Light Sources and Light Sensing Devices.

The light sources and light sensing devices were mounted as shown in Fig. 3. Two matched phototransistors (Philips OCP71) were mounted in an aluminum block through which water from a 25°C thermostat was circulated. The electronic circuits associated with the phototransistors were mounted inside an aluminum box attached to the phototransistor mounting block. The entire assembly was insulated with styrofoam. The photoelectronic circuits are shown in Fig. 4.

c. Measurement of Weight Change.

The null, or reference position of the balance, was determined as a zero reading on the phototransistor circuit galvanometer (Fig. 4); and the voltage in the potentiometer circuit (Fig. 5) necessary to attain this position of the balance beam was recorded as the reference voltage. Weight change in the sample was measured as the difference in voltage necessary to restore the balance beam to the null position.

d. Pressure Measurement.

Pressures greater than 1.5 torr were measured with a U-type mercury manometer. Pressures less than this were measured with a spoon gauge as described by Machin (26). The electronic circuit associated with the spoon gauge is shown in Fig. 6. An audio oscillator (GR Type 1311-A) supplied the primary winding of the differential transformer (Schaevitz Engineering 100-A1) with a 1 kHz signal. The outputs of the differential transformer were rectified by diodes (Phillips OA10) mounted in an aluminum block thermostated at 25°C. The bridge circuit was balanced using a decade resistor (GR Type 1432 T). A recording galvanometer (YSI Model 81), with a sensitivity of 10 mv full scale, was used as null detector. The maximum sensitivity of the gauge was  $2.5 \times 10^{-3}$  torr.

The zero point of the spoon gauge was checked periodically by isolating the gauge from the line and freezing the vapour from the gauge with a liquid nitrogen trap.

A sensitive cathetometer was used to read the mercury manometer.

The spoon gauge was calibrated against an oil manometer to pressures of 11.5 torr, and against a mercury manometer in the range of pressures from 11.5 to 13.0 torr. The calibration procedures are described in Appendix 1. The pressure in the vacuum line was related directly to the value of resistance necessary

to balance the voltage across the recorder (See Fig. 6). The values of pressure and corresponding resistances are listed in Appendix 1, Table 2, and plotted in Appendix 1, Fig. 3. Pressure values were corrected to account for the temperature dependence of the densities of mercury and oil.

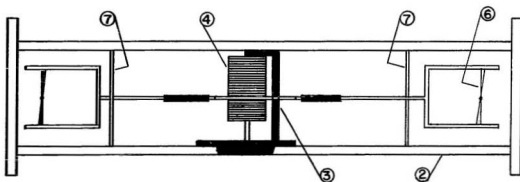
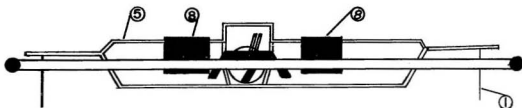
e. Thermostated Bath.

A bath was used to thermostat the sample at temperatures of  $20^{\circ}\text{C}$ ,  $5.8^{\circ}\text{C}$ , and  $-7.45^{\circ}\text{C}$ . The bath regulated within  $\pm 0.02$  C of the set temperatures. Water was used in the bath at  $20^{\circ}\text{C}$  and  $5.8^{\circ}\text{C}$ , while a mixture of 2/3 ethanol and 1/3 water was used at  $-7.45^{\circ}\text{C}$ . Tap water was used as coolant, except at  $-7.45^{\circ}\text{C}$ , for which methanol at ca.  $-15^{\circ}\text{C}$  was used.

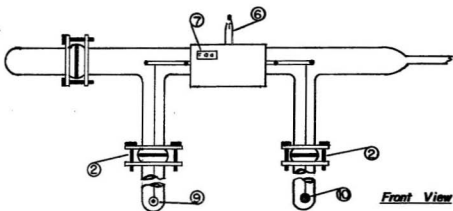
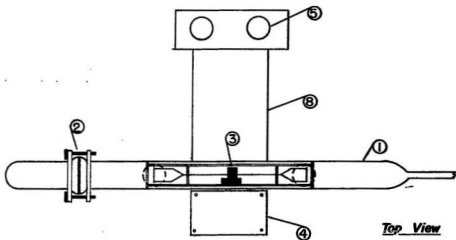
The bath was filled, brought to temperature, and allowed to equilibrate for four hours before starting a run.

3. Calibration of the Balance.

Archimedes' Principle was used to calibrate the balance (16). The apparent mass change of a glass bulb was measured as a function of the pressure of trichlorofluoromethane in the system. The large bulb was replaced by a glass bead and the measurements were repeated. The sensitivity was calculated using the formula (16):

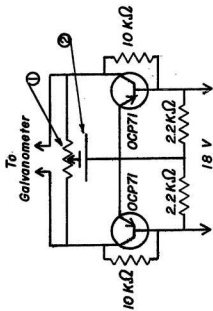
Balance Beam Assembly.Top ViewFront ViewLegend

- ① Hangdown of Quartz Hooks.
- ② Frame of 2 mm. Quariz Rods.
- ③ Microammeter Movement.
- ④ Moving Coil of Microammeter Movement.
- ⑤ Balance Beam.
- ⑥ Tungsten Wire Supports for Hangdowns.
- ⑦ Arrests.
- ⑧ Aluminum Foil Vanes .

FIGURE — 3Overall Balance AssemblyLegend

- ① Balance Case.
- ② "O" Ring Seals.
- ③ Balance Arm Assembly.
- ④ Aluminum Box Containing Phototransistor and Circuits.
- ⑤ Light Sources (60 watt bulbs).
- ⑥ Connection to Balance Beam Circuit.
- ⑦ Connections to Phototransistor Circuits.
- ⑧  $\frac{1}{2}$ " Plywood Support.
- ⑨ Sample Bulb.
- ⑩ Counterweight.

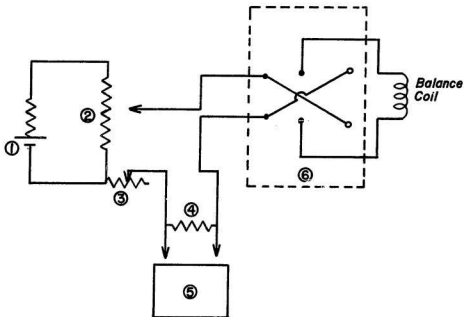
FIGURE - 4



Legend

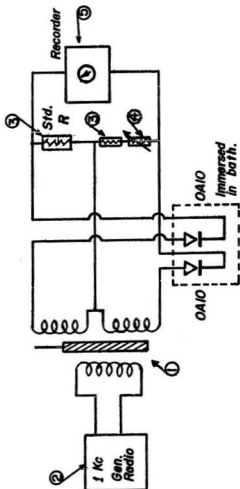
- ① Potentiometer  $10\text{ K}\Omega$  (Bourne Trimpot H-41)
- ② Regulated Voltage Supply (Technipower PC 23.3 - 0.100)

Photo Transistor Circuit

Legend

- ① Regulated Power Supply ( 6V Technipower MC 6.0-0.500v  
± 0.05 % )
- ② Coarse Control ( Bourns 1 K $\Omega$  10 turn potentiometer )
- ③ Fine Control ( " " " " " " )
- ④ Standard Resistances ( Gen. Radio 500  $\Omega$  ± 0.025 %  
Type 500 - F )
- ⑤ Potentiometer.
- ⑥ Reversing Switch.

FIGURE-6



Legend

- ① Differential Transformer (Schaevitz Engineering 100-A1)
- ② Audio Oscillator (GR Type 1311-A)
- ③ Standard Resistances (K $\Omega$ , GR Type 500 H)
- ④ Decade Resistor (GR Type 1432 T)
- ⑤ Recording Galvanometer (YSI Model 81)

Semi-Schematic Diagram of Spoon Gauge Circuit.

$$S = \frac{M(V_1 - V_2) 10^6}{(S_1 - S_2) 2 PV} \dots\dots (2)$$

$$S = \mu\text{g}/\mu\text{V}$$

M = Molecular weight of the gas in gm/mole.

$V_1$  = Volume of the buoyancy bulb  $\text{cm}^3$ .

$V_2$  = Volume of the glass bead  $\text{cm}^3$ .

$S_1$  = Slope of the graph of pressure vs weight using the buoyancy bulb  $\mu\text{V}/\text{mm}$ .

$S_2$  = Slope of the graph of pressure vs weight change for the glass bead.

$$P = 76$$

$$V = -22,400 \text{ cm}^3 \text{ per mole}$$

Z = Temperature correction to operating temperature.

The calibration data and graphs are in Appendix 2.

The slopes of the graphs were calculated using least squares. The average of the slopes of the graphs obtained with the buoyancy bulb was  $(-1.024 \pm .00084) \times 10^{-2}$ . The average of the slopes of the graphs obtained with the buoyancy bulb was  $(-0.0015 \pm .00007) \times 10^{-2} (\text{v}/\text{cm})$ .

Using Equation 2, the sensitivity was calculated to be 39.54  $\mu\text{g}/\text{mv}$ .

Twenty divisions on the galvanometer scale corresponded to 0.9 mv. The galvanometer could be read to the nearest 0.5 divisions. This corresponds to 0.027 mv which was less than the accuracy to which voltage could be measured. The accuracy of reading on the potentiometer was  $\pm 0.05$  mv corresponding to an error of ca. 2.0  $\mu\text{g}$ . The weight change of the sample was measured as a difference between two voltages read from the potentiometer, hence the experimental error in measuring a weight change was  $\pm 4.0$   $\mu\text{g}$ . For the adsorbates used in this study, this corresponded to  $\pm 0.03$ .

The buoyancy of the sample was checked in situ by admitting air through a dry ice trap into the balance to a pressure of 400 mm and observing any weight change. None was observed.

#### 4. Vacuum Line.

A schematic drawing of the vacuum line is given in Fig. 7. Metal valves were used in the equilibrium section of the line since tetrachloroethylene is very soluble in stopcock grease.

## 5. Materials.

The adsorbent used during this study was anhydrous nickel sulfate. The adsorbates used were tetrachloroethylene and trichlorofluoromethane.

Tetrachloroethylene (Eastman Kodak Spectro Grade, Lot 10C) was placed on the vacuum line and degassed by freezing with a dry ice-ethanol mixture, pumping off any gas over the solid, and thawing. This cycle was repeated on each sample taken until no bubbles formed in the liquid during thawing, and the pressure over the solid after refreezing was less than 3 microns. The sample was then triply distilled in vacuum, at room temperature, into a receiving vessel cooled with a dry ice-ethanol mixture. The middle fraction of each distillation was kept; the head and tail fractions were discarded.

Trichlorofluoromethane (Matheson, purity of 99.5 mole per cent) was purified in the same manner, except that each sample was doubly rather than triply distilled; and liquid nitrogen was used as a coolant. The physical configuration of the vacuum line made it impossible to triply distill the trichlorofluoromethane.

The saturated vapour pressure of the adsorbates was measured at the experimental temperatures. The values obtained are given in Table 1. The graph of  $\log P$  vs.

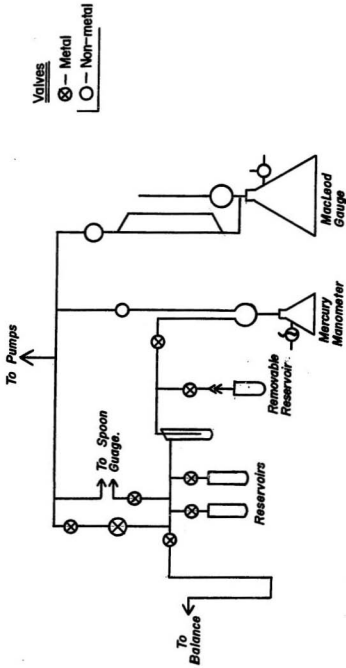
$\frac{1}{T}$  is in Appendix 3.

T

TABLE 1

Vapour Pressures  
of Tetrachloroethylene and Trichlorofluoromethane

Temp. (°C)	Vapour Pressure (mm Hg)	
	Tetrachloro- ethylene	Trichlorofluoro- methane
20.0	13.82	666.23
5.8	6.0	385.02
-7.45	2.45	215.98

Schematic Diagram of the Vacuum Line.

Anhydrous nickel sulphate was prepared from the hexahydrate (Fisher Reagent Grade) by dehydration in situ in the balance. The sample was pumped at room temperature until no weight change was evident over a 12 hour period. The sample then was pumped and heated at approximately  $10^{\circ}$  intervals from  $30^{\circ}\text{C}$  to  $120^{\circ}\text{C}$ . The sample was heated at each intermediate temperature for a 24 hour period, and at  $120^{\circ}\text{C}$  for two days, after which time no further loss of weight occurred. The sample was not heated above  $120^{\circ}\text{C}$  to avoid the possible decomposition of the nickel sulfate. The weight of the anhydrous nickel sulfate sample was 0.452 gm.

#### 6. Experimental Procedure.

Adsorption points were obtained by slowly introducing a small amount of adsorbate from the storage bulb into the system and equilibrating until the sample weight became constant. At relative pressures of less than 0.5, about five minutes were required for equilibration. The time required to reach equilibration at pressures above this level increased to ca. four hours near the saturation vapour pressure. Desorption points were obtained by condensing the vapour into a reservoir immersed in liquid nitrogen for the trichlorofluoromethane and dry ice-ethanol mixture for the tetrachloroethylene.

Pressures were measured with the mercury manometer or spoon gauge or, in regions where the gauges overlap, with both gauges.

## EXPERIMENTAL RESULTS

The data for the adsorption and desorption runs are tabulated in Appendix 4. The isotherms corresponding to this data are in Figures 8 to 13.

## DISCUSSION

### 1. The Isotherms.

The isotherms of tetrachloroethylene and trichlorofluoromethane, shown in Fig. 8 to 13, are of Type B according to the classification of deBoer(9) as shown in Fig. 1. The upper closure point is asymptotic with saturation vapour pressures of the adsorbates. The lower closure point of the first adsorbate occurs at low relative pressures and displays a well-defined shoulder. The regions of the adsorption branches of the curves near the shoulders were reproducible and independent of the amount adsorbed. The regions at relative pressures above the shoulder points, however, depended upon the amount adsorbed prior to beginning desorption. The region in which the curves were reproducible was determined by starting desorption from various amounts adsorbed. It was necessary to adsorb a large excess of adsorbate in order to obtain a reasonably extended reproducible region in the desorption curve.

FIGURE - 8

Isotherm for Tetrachloroethylene on Nickel Sulfate at 20.0°C.

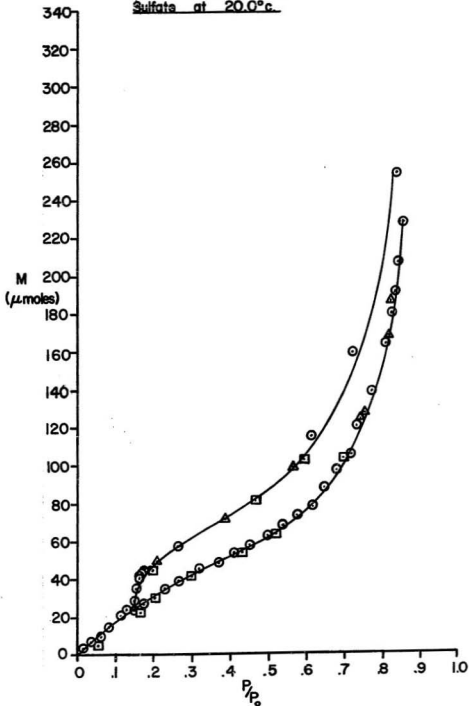
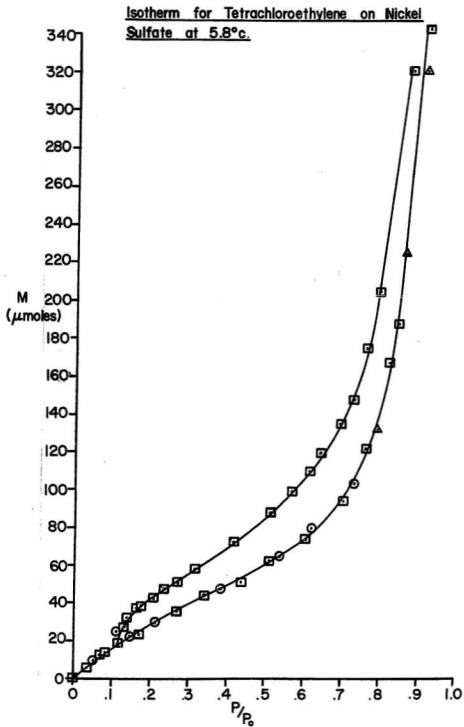


FIGURE - 9

35  
FIGURE - 10

isotherm for Tetrachloroethylene on Nickel  
Sulfate at -7.45°C.

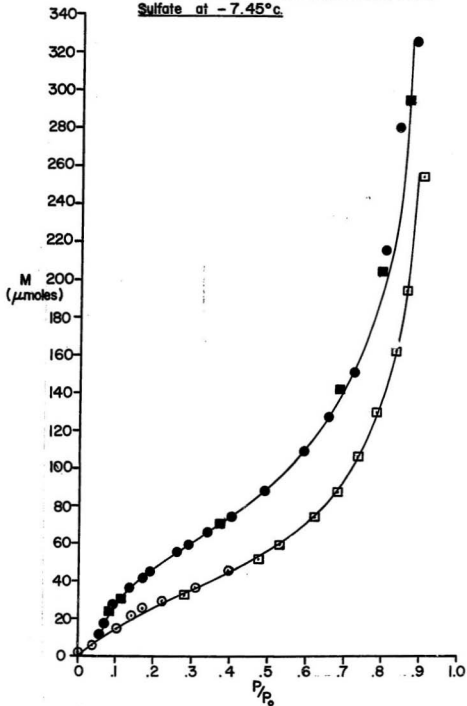


FIGURE - II

Isotherm for Trichlorofluoromethane on Nickel Sulfate at 20°C.

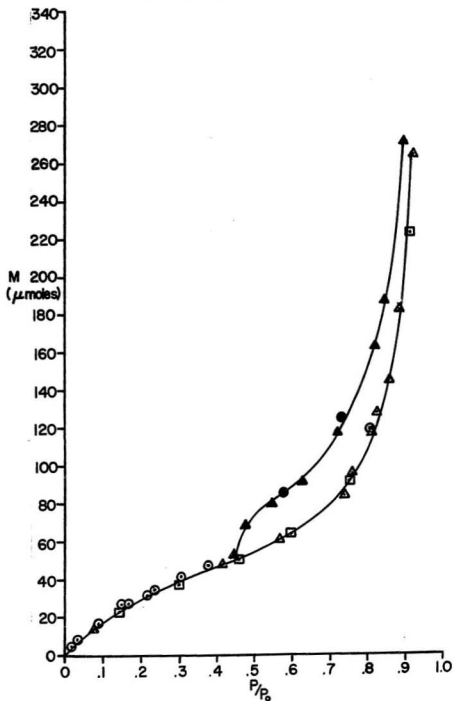


FIGURE - 12

Isotherm for Trichlorofluoromethane on Nickel Sulfate at 1.0°C.

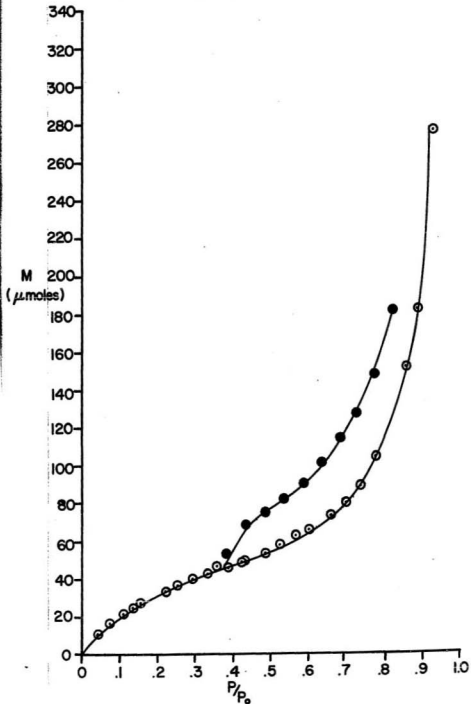
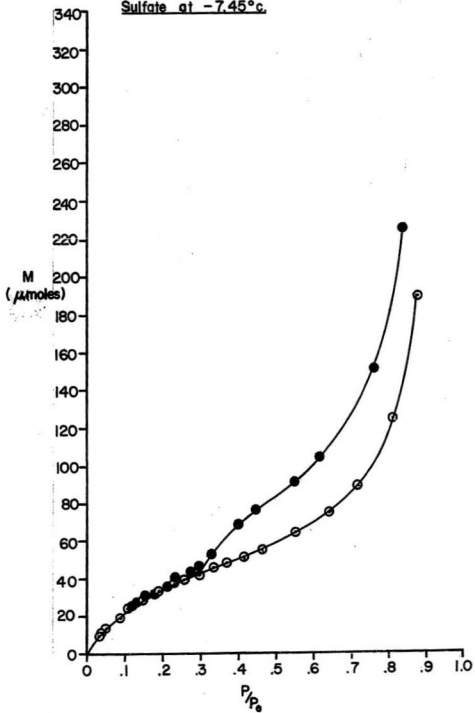


FIGURE 13

Isotherm for Trichlorofluoromethane on Nickel Sulfate at  $-7.45^{\circ}\text{C}$ .



These isotherms are similar to those obtained by Barrer and MacLeod (7) with nitrogen, oxygen, and benzene adsorbed on sodium rich montmorillonites. These workers found that the path of the desorption curves was dependent upon the amount adsorbed and suggested that the desorption curves were scanning curves rather than boundary curves. This behaviour is similar to that of the present case.

The results suggest that anhydrous nickel sulfate has a structure similar to that of the montmorillonite clays; that is, that the pores consist of spaces between parallel plates. The lack of closure as  $p/p^0$  approaches unity suggests that these plates may move apart to accommodate the adsorbate molecules.

## 2. Surface Area and Monolayer Capacity.

### a. Monolayer Capacity.

Surface areas were calculated from the monolayer coverage derived from the BET equation and molecular areas derived from the liquid densities of the adsorbates (24).

The BET equation may be written (12)

$$\frac{P}{M_m(P_0 - P)} = \frac{1}{M_m C} + \frac{C-1}{M_m C} \frac{P}{P^0} \dots\dots (2)$$

where  $P$  is the pressure of the adsorbate,  $P^0$  the saturated vapour pressure of the adsorbate, and  $c$  is a constant.

The monolayer capacity,  $M_m$ , may be determined from a plot

of  $\frac{P}{M_m(P^0 - P)}$  against  $P/P^0$ . If  $s$  is the slope of the graph, and  $i$  is the intercept, then;

$$M_m = \frac{1}{S + i} \quad \dots\dots (3)$$

The graphs obtained for tetrachloroethylene and trichlorofluoromethane are in Appendix IV. The slopes of the graphs were determined by least squares. The monolayer capacities are tabulated in Table 2.

b. Surface Area.

The surface area corresponding to monolayer coverage may be calculated from the equation (13),

$$A = M_m B N \times 10^{-26} \quad \dots\dots (4)$$

$A$  = area of the surface ( $m^2$ ).

$M_m$  = monolayer capacity ( $\mu$  moles).

$B$  = molecular area ( $\text{\AA}^2$ ).

$N$  = Avogadro's number.

If it is assumed that the molecular packing and configuration of adsorbate molecules on the surface are those which occur in bulk liquid phase of the adsorbate, then the molecular area may be calculated from equation (27)

$$B = f \left( \frac{W}{\rho N} \right)^{2/3} \cdot 10^6 \quad \dots\dots (5)$$

TABLE 2

Monolayer Capacities and Surface Area  
of Anhydrous Nickel Sulfate

Adsorbate

Temp. (°C)	<u>Tetrachloroethylene</u>		<u>Trichlorofluoromethane</u>	
	Monolayer Capacity ( $\mu$ moles)	Area ( $m^2$ )	Monolayer Capacity ( $\mu$ moles)	Area ( $m^2$ )
20	45.54	9.17	36.93	6.93
5.8	44.39	8.94	34.42	6.46
-7.45	42.47	8.55	36.39	6.83
Average values	44.1	8.88	35.9	6.74

- $B$  = apparent molecular area ( $\text{\AA}^2$ ).  
 $W$  = molecular weight of adsorbate.  
 $N$  = Avogadro's number.  
 $\rho$  = density of adsorbate.  
 $f$  = packing factor 1.091 if each molecule has 12 nearest neighbours.

The densities of the adsorbates were found to be (24):

Tetrachloroethylene	1.494 gm cm <sup>-3</sup>
Trichlorofluoromethane	1.623 gm cm <sup>-3</sup>

Using the above densities, equation (5) gave the following molecular areas

Tetrachloroethylene	-33.4 $\text{\AA}^2$
Trichlorofluoromethane	-31.2 $\text{\AA}^2$

The surface areas calculated from these values are summarized in Table 2.

### 3. Heats of Adsorption.

Crowell and Young (12) show that for isothermal adsorption systems, and isosteric heat of adsorption,  $q_{st}$  is described by;

$$q_{st} = RT^2 \left( \frac{\partial}{\partial T} \ln P \right)_{n_s} = -R \left( \frac{\partial}{\partial (1/T)} \ln P \right)_{n_s} \dots (6)$$

where  $n_s$  refers to the number of moles adsorbed.

It follows from equation (6) that the slope of a graph of pressure against  $1/T$ , at constant coverage, multiplied by  $R$  yields the isosteric heat. The isosteric heats at various fractions of surface coverage, of adsorbed tetrachloroethylene and trichlorofluoromethane during adsorption and desorption, calculated using least squares, are tabulated in Appendix 6, and plotted in Figure 4.

The average heat of vaporization of the adsorbates over the experimental temperature range were calculated using an integrated form of the Clausius-Clapeyron equation (28).

$$\log \frac{P_2}{P_1} = \frac{\Delta H_v}{4.576} \cdot \frac{T_2 - T_1}{T_1 T_2} \quad \dots (7)$$

The saturated vapour pressures of the adsorbates are listed in Table 1. The heats of vaporization were calculated to be:

Tetrachloroethylene	9.74 kcal mole <sup>-1</sup>
Trichlorofluoromethane	6.35 kcal mole <sup>-1</sup>

The differential heat of adsorption,  $q_d$ , may be calculated using the expression of Crowell and Young (12)

$$q_d = q_{st} - RT$$

The values of  $q_d$  are also listed in Appendix 6 (8).

The heat curves of both adsorbates decrease as monolayer is approached and reach a minimum in the region of a monolayer coverage. It is not uncommon for systems to show a decrease in the heat of adsorption in the monolayer region (29,30,31), or a minimum in the monolayer region (32). This behaviour is commonly explained in terms of surface heterogeneity (33,13).

The heats of both adsorbates approach the heat of vaporization of the bulk material as coverage increases; the trichlorofluoromethane more quickly than the tetrachloroethylene.

The heat curve of the tetrachloroethylene is different in that its heat is less than the heat of vaporization. This unusual behaviour has been observed in other systems (34).

The heats calculated from the desorption curves are greater than those calculated from the adsorption curves but converge at higher coverages.

#### 4. Entropies of Adsorption.

##### a. Experimental Entropy Change.

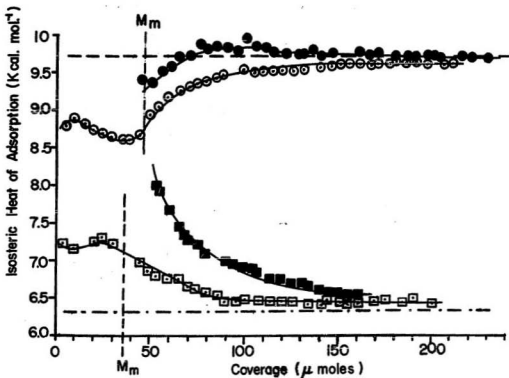
The difference between the molar entropy of a gas,  $S_G$  and the differential entropy of its adsorbed state,  $\bar{S}_S$ , at constant coverage  $n_s$ , and area of adsorbate A, is shown by Young and Crowell (12) to be;

FIGURE-14

Isosteric Heats of Sorption for  
Tetrachloroethylene and Trichlorofluoromethane.

Legend

	<u>Tetrachloroethylene</u>	<u>Trichlorofluoromethane</u>
<u>Adsorption</u>	○	□
<u>Desorption</u>	●	■
<u>Latent Heat of Vaporization</u>	-----	-----
$M_m$	—	—
	Monolayer Coverage	



$$RT \left( \frac{\partial \ln P}{\partial T} \right)_{n_{S,A}} = S'_G - \bar{S}_S$$

When equation (9) is compared to equation (6) it is seen that;

$$S'_G - \bar{S}_S = \frac{q_{st}}{T}$$

where  $q_{st}$  is the isosteric heat of adsorption.

Equation (10) was used to calculate the experimental values of  $(S'_G - \bar{S}_S)$  from the adsorption isotherms of tetrachloroethylene and trichlorofluoromethane. The values of these experimental entropy changes are listed in Appendix 6.

#### b. Theoretical Entropy of Condensation.

The hysteresis in the isotherms suggested that condensation occurred during adsorption. A theoretical entropy change was calculated  $(S'_G - S_L)$  for the condensation of gas to liquid at experimental conditions.

The entropy of the liquid,  $S_L$ , was assumed to be independent of pressure for these calculations. If the standard entropy of the gas is  $S_G^0$  at temperature  $T^0$ , and pressure  $P^0$ , then the entropy of the liquid at temperature  $T$  will be:

$$S_L = S^0 - (S_G^0 - S_L^0) - C_p \ln \frac{T^0}{T} \dots (11)$$

where  $C_p$  is the heat capacity of the liquid and  $(S_G^0 - S_L^0)$

is the entropy of condensation at  $T^{\circ}$ .

To determine the entropy of condensation at experimental conditions it was necessary to calculate the entropy,  $S_G'$ , at experimental conditions. Intergration of the Maxwell Equation

$$\frac{\partial S}{\partial P} \bigg|_T = - \frac{\partial V}{\partial T} \bigg|_P$$

gives

$$S_G' - S^{\circ} = R \ln \frac{P^{\circ}}{P} \quad \dots\dots (12)$$

The entropy of a gas at temperature  $T$  and pressure  $P$  is related to the entropy of the gas at standard conditions by the equation (35);

$$S_G' = S_G^{\circ} + C_p \ln \frac{T}{T^{\circ}} + R \ln \frac{P^{\circ}}{P} \quad \dots\dots (13)$$

where  $C_p$  is the heat capacity of the gas at fixed pressure.

The constants used in conjunction with equations (11) to (13) to calculate the theoretical entropy changes are listed in Appendix 7. The values calculated for the entropies of liquid tetrachloroethylene and trichlorofluoromethane at  $20^{\circ}\text{C}$  are 57.9 eu and 53.41 eu respectively. The calculated values of the gas entropies  $S_G'$ , and the theoretical entropies of condensation ( $S_G' - S_L$ ) are given in Appendix 8.

c. Theoretical Entropy of Two Dimensional Gas.

It was considered possible in the region below monolayer coverage ( $\theta=1$ ) that the adsorbed state may be a two dimensional gas. The statistical description of the translational entropy of a three dimensional gas is given by Glasstone (35);

$$S_G = RT \left( \frac{\partial}{\partial T} \ln Q_3 \right)_V + R \ln Q - K \ln N! \dots (14)$$

where  $Q_3$  is the partition function of a three dimensional gas;

$$Q_3 = \frac{(2\pi mkT)^{3/2}}{h^3} V$$

For a two dimensional gas the entropy is;

$$S_S = RT \left( \frac{\partial}{\partial T} \ln Q_2 \right)_{A-b} + R \ln Q_2 - K \ln N! \dots (15)$$

Where  $Q_2$  is the partition function of a two dimensional gas;

$$Q_2 = \frac{(2\pi mKT)(A-b)}{h^2}$$

The change in entropy associated with transition from a three dimensional gas to a two dimensional,  $S_G - S_S$  gas will be;

$$S_G - S_S = RT \left( \frac{\partial}{\partial T} \ln \frac{Q_2}{Q_3} \right) + R \ln \frac{Q_3}{Q_2} \dots (16)$$

According to Crowell and Young (1),

$$S_S = S_S^- + \frac{R}{1-\theta} = S_S^- + \frac{R}{1-\theta}$$

Substituting this in equation (8) gives;

$$S_G - \bar{S}_S = RT \frac{\theta}{3T} \ln \frac{Q_3}{Q_2} + R \ln \frac{Q_3}{Q_2} + \frac{R}{1-\theta}$$

Simplifying and differentiating the partition function;

$$S_G - \bar{S}_S = \frac{R}{2} \ln(2\pi mKT) + R \ln h V(A-b) + \frac{R}{1-\theta} \dots (17)$$

From the ideal gas law;

$$V = \frac{RT}{P}$$

which becomes,  $R \ln V = R \ln KT$

if the standard conditions are set at 1 atmosphere.

Substitution of this in equation (17) gives;

$$S_G^0 - \bar{S}_S = \frac{R}{2} \ln(2\pi mKT) + R \ln hRT + \ln(A-b) + \frac{R}{1-\theta} \dots (18)$$

A, in these equations is the area available per molecule,

b is the area of the molecules themselves. It follows (1)

that

$$\frac{A-b}{A} = 1 - \frac{b}{A} = 1 - \theta$$

$$A = b/\theta$$

$$\ln(A-b) = \ln b - \ln \frac{\theta}{1-\theta}$$

Substituting this in equation (10) gives;

$$S_G^0 - \bar{S}_S = \frac{3}{2}R \ln T + \frac{R}{2} \ln(2\pi mK) + R \ln \frac{Rhb\theta}{1-\theta} \dots (19)$$

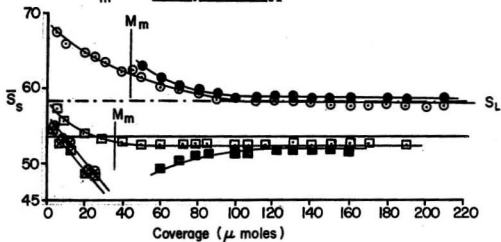
FIGURE - 15

Entropy of Adsorbed State ( $\bar{S}_s$ ) for Tetrachloroethylene  
and Trichlorofluoromethane at 20°C.

Legend

	Tetrachloroethylene	Trichlorofluoromethane
$\bar{S}_s$ Ads	○	□
$\bar{S}_s$ Des	●	■
$S_{\text{liquid}}$	- - - - -	—————
$\bar{S}_s$ 2D gas	⊙	⊠

$M_m$  — Monolayer Coverage



This is the equation for the theoretical entropy change associated with the conversion of three dimensional gas at standard conditions to a two dimensional gas at coverage  $\theta$ . If  $S_G^0$  is known, the theoretical entropy  $\bar{S}_S$  of the two dimensional gas may be calculated from equation 19.

These values were calculated for tetrachloromethylene and trichlorofluoromethane and are listed in Appendix 10 and plotted in Figure 15.

The comparisons of the theoretical to the experimental entropies assume that the entropy changes are predominantly translational. The difference between experimental and theoretical entropies of the tetrachloroethylene may be due to the appearance of a weak vibration perpendicular to the surface.

##### 5. Capillary Condensation.

As previously mentioned, the general features of the adsorption-desorption isotherms suggest that the hysteresis is caused by condensation of the adsorbate in parallel plate capillaries. The entropy calculations (Figure 15) also suggest that adsorbates are liquid-like in the region of hysteresis.

Using a model in which the adsorbent consists of parallel plates which may move apart to accommodate adsorbent molecules, it is possible to derive a form of the Kelvin equation which describes both the adsorption and desorption branches of the isotherms. Information may

also be obtained concerning the contact angle of the adsorbate and adsorbent, and the thickness of the adsorbed layer which does not participate in the formation of the meniscus.

In the case of condensation between parallel plates, the Kelvin Equation becomes;

$$\ln \frac{P}{P^0} = - \frac{v_m \gamma \cos \theta}{r RT} \quad \dots (20)$$

$v_m$  = molar volume of the liquid

$\gamma$  = surface tension of the adsorbate

$r$  = radius of curvature of the meniscus

$R$  = universal gas constant

$T$  = temperature

$\theta$  = contact angle

The molar volume,  $v_m$ , may be related to the area of the adsorbent by

$$v_m = B \delta N \quad \dots (21)$$

$B$  = molecular area.

$N$  = Avogadro's number.

$\delta$  = effective diameter of the adsorbate molecules.

Substituting (21) into (20) gives;

$$\ln \frac{P}{P^0} = - \frac{\gamma \cos \theta}{r RT} \cdot B \delta N$$

The radius of curvature of the meniscus will not be the radius of the pore. The pore radius will be reduced as a number of layers,  $x$ , of adsorbate will be adsorbed on the pore surface but will not participate in the formation of the meniscus. This layer will also remain after evaporation (13). The radius of curvature may be related to the total number of adsorbed layers of molecules,  $\theta$ , by;

$$r = S (\theta - X)$$

which when substituted into equation (22) along with equation (21) gives

$$\ln \frac{P}{P^0} = - \frac{\gamma \cos \phi}{RT} \cdot \frac{B N}{\theta - X} \quad \dots (23)$$

Inverting (23) gives

$$\frac{-1}{\ln \frac{P}{P^0}} = \frac{RT}{BN \gamma \cos \phi} (\theta - X)$$

which is the equation of a straight line provided  $(\gamma \cos \phi)$  is constant;

The slope,  $S$ , of this line will be;

$$S = \frac{-RTM_m}{A \gamma \cos \phi} \quad \dots (25)$$

and the intercept,  $i$ , will be;

$$i = \frac{RTM_m}{A \gamma \cos \phi} \cdot X \quad \dots (26)$$

The value of  $x$  may be derived from equation (24) since  $x = \theta$  when

$$\frac{-1}{\ln \frac{P}{P^0}} = \theta \quad \dots (27)$$

Values of  $\frac{1}{\log \frac{P}{P^0}}$  and  $\theta$  were calculated and are given in Appendix 11. The corresponding graphs are plotted in Figures 16, 17, and 18. The slopes, intercepts and  $x$  values were calculated from the linear portions of the graphs and are given in Table 3.

In order to calculate the contact angle  $\beta$ , the values of  $\gamma \cos \beta$  were calculated from the slopes of the graphs. The surface tensions,  $\gamma$ , of the adsorbates at experimental temperatures were calculated from the Guggenheim equation (37)

$$\gamma = \gamma^0 \left(1 - \frac{T}{T_c}\right)^{11/9} \quad \dots (28)$$

$T$  = temperature .

$T_c$  = critical temperature .

Values of  $\gamma^0$  were chosen such that equation (28) gave the correct values of surface tensions of the adsorbates at 20°C. The values calculated for  $\gamma$  are in Table 4. The critical temperatures of the adsorbates are (37).

Tetrachloroethylene	347.1° C
Trichlorofluoromethane	471.2° C

The values of  $\gamma \cos \beta$  and  $\beta$  are reported in Table 5.

The linear portions of the adsorption and desorption curves in Figures 16, 17, 18 indicate the regions in which the adsorbate is behaving as a liquid with the term  $(\gamma \cos \theta)$  a constant. For trichloromethane, this corresponds roughly to the section of the entropy curve (Figure 15) where  $\bar{S}_S = S_L$ . But for the tetrachloroethylene this is not the case: the Kelvin plot becomes linear in the region of 1 monolayer, but  $\bar{S}_S \neq S_L$  until a coverage of ca. 2 1/2 monolayers is reached. The intermolecular interactions of the tetrachloroethylene would seem to be strong enough that the adsorbed aggregate of molecules behave as a liquid before the spacial crowding is such that the restriction on the degrees of freedom of the molecules is that within the normal liquid. That the intermolecular forces in the tetrachloroethylene are greater than those in the trichlorofluoromethane is indicated in some measure by the greater surface tension of the former. The inverted Kelvin equation plots indicate liquid behaviour for both of the adsorbates before the heats of adsorption equal the latent heats of fusion of the adsorbates (Figure 18). In addition to the effects of intermolecular forces, premature appearance of liquid behaviour as indicated by the Kelvin equation may also be due to the confinement of the adsorbate molecules within the very small pores.

It was suggested previously that the adsorbent consists of plates that may move apart to accommodate

TABLE 3

Slopes, Intercepts and "X" Values of Inverted  
Kelvin Equation Plots

Tetrachloroethylene

Temp. (°C)	<u>Adsorption</u>			<u>Desorption</u>		
	Slope	Intercept	X	Slope	Intercept	X
20	3.331	-1.341	.402	2.590	-1.967	.759
5.8	3.516	-1.499	.426	2.486	-1.541	.619
-7.45	3.805	-1.45	.381	2.768	-2.523	.905
			<u>.403</u>			<u>.761</u>
	Average "X"					

Trichlorofluoromethane

Temp. (°C)	<u>Adsorption</u>			<u>Desorption</u>		
	Slope	Intercept	X	Slope	Intercept	X
20	4.276	-2.877	.672	3.130	-3.160	1.009
5.8	3.960	-2.50	.631	3.229	-4.018	1.224
-7.45	3.872	-2.682	.692	3.018	-4.097	1.357
			<u>.665</u>			<u>1.193</u>
	Average "X"					

TABLE 4

Values of Surface Tension of Adsorbates  
Calculated from the Guggenheim Equation

Temp. (°C)	Surface Tension ( $\gamma$ )	
	Tetrachloro- ethylene	Trichlorofluoro- methane
20	36.74	19.5
5.8	33.29	21.4
-7.45	34.85	23.1

TABLE 5

Values of  $\gamma \cos \phi$ ,  $\cos \phi$  and  $\phi$  Calculated from  
Inverted Kelvin Equation Plots

Tetrachloroethylene

Temp. (°C)	<u>Adsorption</u>			<u>Desorption</u>		
	$\gamma \cos \phi$	$\cos \phi$	$\phi$	$\gamma \cos \phi$	$\cos \phi$	$\phi$
20	8.378	.264	74.3 <sup>o</sup>	10.785	.339	70.2
5.8	7.552	.227	76.9	10.682	.321	71.2
-7.45	6.645	.191	79.0	9.136	.262	74.8

Trichlorofluoromethane

Temp. (°C)	<u>Adsorption</u>			<u>Desorption</u>		
	$\gamma \cos \phi$	$\cos \phi$	$\phi$	$\gamma \cos \phi$	$\cos \phi$	$\phi$
20	6.986	.358	69.5 <sup>o</sup>	9.541	.489	60.7
5.8	7.179	.336	70.4	8.804	.411	65.8
-7.45	6.992	.303	72.4	8.970	.388	67.2

adsorbent. If this is the case, the radius of curvature of the menisci of adsorbate condensed in the pores must change as adsorption progresses. Theoretical considerations suggest that the surface tension of a liquid is a function of the radius of curvature (38). It is seen however, that  $(\gamma \cos \theta)$  is constant over the range of the inverted Kelvin equation plots which suggest that either the surface tension of the adsorbate is independent of the radius of curvature over the range of the Kelvin equation plots or that there are factors which compensate for any changes in surface tension.

In a system consisting of plates that can move, condensation will first occur when a quantity of adsorbate is sufficient to bridge the space between the plates. As adsorption progresses, more adsorbate will condense between these plates which can move apart. In addition, condensation will occur between plates of greater separation. During desorption as liquid is lost from between the plates, the plates may move closer together. At the point at which the plates reach their minimum separation, the cylindrical meniscus will recede until there is insufficient adsorbate to maintain it. The adsorbate will then separate into unjoined layers on the faces of the capillary space. It may be possible for the plates to be drawn closer together than they are in adsorbate free state, in which case capillary condensation will persist to coverages lower than that where condensation began. If such de-

58  
FIGURE -16

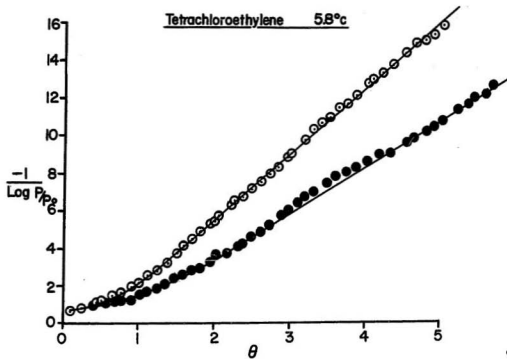
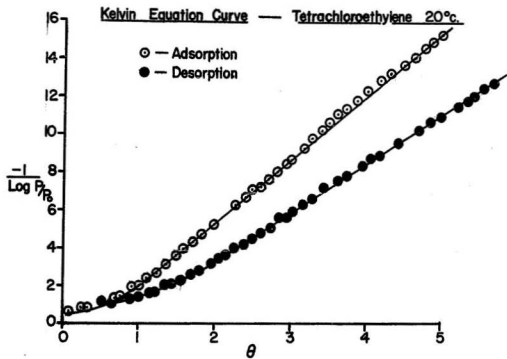


FIGURE - 17

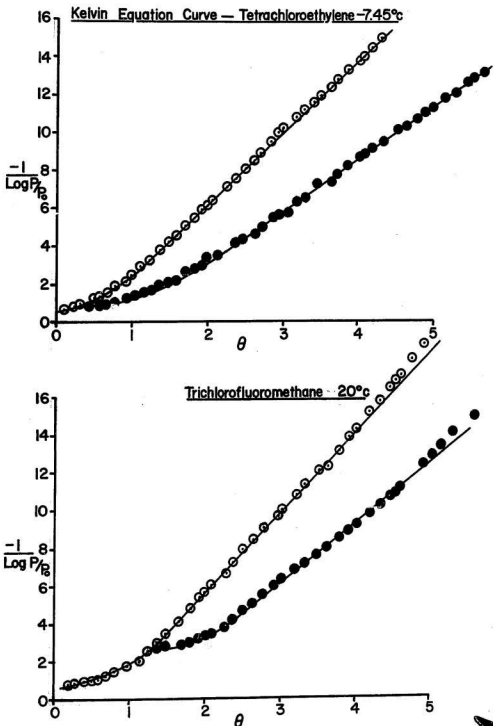
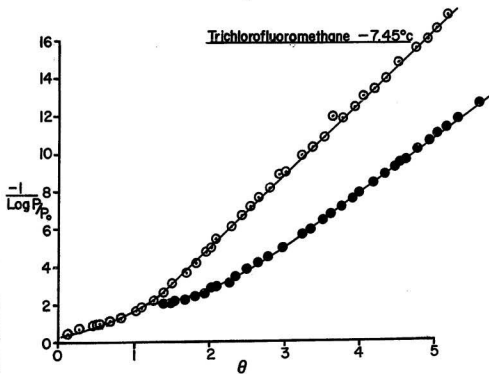
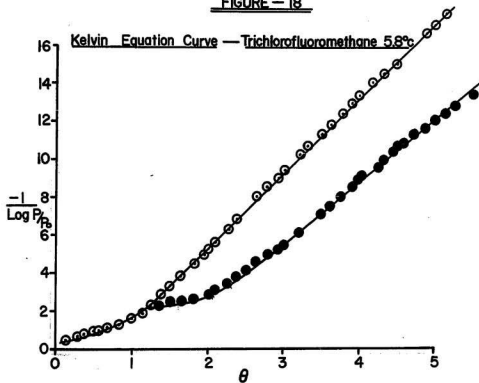


FIGURE - 18

formation cannot occur, then it should be impossible for condensation to persist in this manner; and the lower closure point ought to correspond to the point at which condensation began.

The closure points for both adsorbates correspond approximately to the calculated values of  $x$ . The closure point of the trichlorofluoromethane are close to the point where liquid behaviour begins. But the closure point of the tetrachloroethylene closure point persists to a value of  $\theta$  below the point where condensation appears to begin. The fact that this occurs for only one of the adsorbates used may be the result of the high surface tension of the tetrachloroethylene relative to that of the other adsorbate.

The pores would seem to be very small; the distance between the plates being in the region of 2 monolayers, or ca.  $12 \overset{\circ}{\text{A}}$  apart.

It is particularly interesting that the adsorbate exhibits liquid like behaviour at such low coverages. The Kelvin equation is adhered to at coverages of 2 monolayers which corresponds to a film of 4 layers of adsorbate molecules between the plates of adsorbents.

The adsorption branches of the inverted Kelvin equation plots are approximately linear below the region where condensation seems to occur.

This suggests that the adsorbates are adhering to an equation of the form of the universal nitrogen isotherms as proposed by Pierce (39),

$$n^{2.75} = - \frac{1.30}{\log \frac{P}{P_0}} \quad \dots (29)$$

in which the power of the exponent is 1 rather than 2.75. The universal isotherm has been used to detect condensation. This presumes that the film of adsorbate not condensed in the pores has no liquid like properties. It is seen in the present study that liquid like properties may exist in very thin films of adsorbate.

SUMMARY

When tetrachloroethylene and trichloro-fluoromethane are sorbed on anhydrous nickel sulfate, condensation occurs. As coverage increases, the adsorbent expands to accommodate more adsorbate.

Values were calculated for the heats of adsorption and for the entropies of the adsorbed states. Values were also calculated for the latent heats of vaporization of the adsorbates, and for the entropies of the adsorbates in the liquid states as well as in the two-dimensional gas state. The comparison of these values indicated that condensation occurred at coverages in the region of ca. two to two and a half monolayers for both adsorbates. However, analysis with the Kelvin equation indicated that both adsorbates begin to exhibit liquidlike properties at coverages in the region of one monolayer during adsorption. It would seem that films of adsorbate of a thickness of only two monolayers may exhibit liquid-like properties when confined in the capillary spaces of the adsorbent.

The inverted form of the Kelvin equation used is similar in form to the universal isotherm suggested by Pierce (39)

$$n^{2.75} = \frac{1.30}{\log \frac{p_0}{p}} \quad \dots (29)$$

Equation (29) differs from equation (24) in that the power of the exponent is 2.75 in the former, and 1 in the latter. The linearity of the inverted Kelvin plots

in Figures 16,17, 18 suggests that the adsorbents may be following a universal isotherm of the type suggested by Pierce but with an exponent of 1.

The universal isotherms have been used to detect capillary condensation (29,40). This application assumes that films adsorbed on surfaces cannot exhibit any liquid like properties such as surface tension. However it is seen from this study that very thin films of adsorbate can display liquid like behaviour which would cause a deviation from the ideal isotherm. While the behaviour observed occurred in capillaries, it is not unreasonable to suggest that films adsorbed on surfaces not within capillaries could display liquid like properties.

Some suggestions for further work are:

1. Determination of the structure of the anhydrous nickel sulphate. X-ray studies (40) have indicated only that the adsorbate has a structure typical of amorphous substances.
2. Calorimetric studies to determine the heats of adsorption in the "shoulder" regions of the desorption isotherms.
3. Study of the time taken to reach equilibrium, particularly at higher coverages where this time is quite considerable. This time may be related to the rates of diffusion or flow of vapour or liquid through the capillary spaces.

4. Studies with a variety of adsorbates to establish dependence of the shape of the isotherm upon the shape of the molecule, the polarity and the surface tension of the adsorbate molecules.

5. Studies with adsorbents known to have capillaries composed of spaces between parallel plates with the present adsorbates.

LITERATURE CITED

1. S.Brunnauer, L.S.Demming, W.S. Demming, and E. Teller; J.Am.Chem.Soc.1940,62,1723.
2. S.Brunnauer, P.H.Emmett and E.Teller; J.Am. Chem.Soc. 1938,60,309.
3. R.Zsigmondy; Z.Anorg.Allgem.Chem.71,356(1911).
4. Treatise on Physical Chemistry, E.O.Kraemer, H.S.Taylor ed. (D.Van Nostrand, New York)1931.
5. J.W.McBain; J.Am.Chem.Soc. 1935,57,697.
6. J.Y.deBoer et al; Kininkl Ned.Akad.Welenship Proc. 1954,1357,170.
7. R.M.Barrer and D.M.McLeod; Trans.Far.Soc. 1954, 50,980. Trans.Far.Soc.1955,51,1290.
8. A.B.C.van Doorn; Graphitoxide; Thesis (1957) Delft.
9. The Structure and Properties of Porous Materials; J.H.deBoer (1957) Butterworths, London.
10. R.M.Barrer, N.M.MacKenzie and J.S.Reay; J.Colloid Sci. II, 1956, 479.
11. The Solid Gas, Interface Vol. II., Dp#1055, D.H. Everett, E.A. Flood ed., (M.Dekker, New York)1961.
12. Physical Adsorption of Gases; D.M.Young and A.D. Crowell; (Butterworths, London) 1962.
13. Adsorption, Surface Area and Porosity; S.J.Gregg and K.S.W.Singh, (Adaemic Press, London) 1967.

14. J.M.Thomas and Brian R. Williams; Quart.Reviews, 19, no.3,23 (1965).
15. Introduction to the Principles of Heterogeneous Catalysis; J.M.Thomas and W.J.Thomas (Academic Press, London), 1967.
16. Vacuum Microbalance Techniques, Vol.1; J.M. Honig, ed. M.J.Katz (Plenum Press, New York),1961.
17. J.W.McBain and A.M.Baker; J.Am.Chem.Soc.1926,48,690.
18. S.Joseforitz and F.F.Othner; Industrial Eng.Chem. 1942, 40,739; D.F.Othmer and F.G.Saurger; Industrial Eng.Chem. 1944,36,894.
19. R.M.Dell and V.J.Wheeler; A.E.R.E. Report # 3425(1960).
20. A.W.Czanderna and I.M.Honig; Analyt.Chem.1957,29,1206.
21. W.D.Machin; Ph.D.thesis (1961), Rensselaer Polytechnic Institute.
22. J.L.Hobs and A.R.Turner; Laboratory Practice, Jly. 1956.
23. Vacuum Microbalance Techniques, Vol. 3; L.Cahn and H.R.Schultz; ed. K.H.Behrndt, (Plenum Press, New York)1962; op cit. Vol. 4, A.Longer, ed. P.M.Waters (Plenum Press, New York)1964.
24. Handbook of Chemistry and Physics; 48th ed. (Chemical Rubber Publishing Company, 1968).
25. Vacuum Microbalance Techniques, Vol. 1, R.F. Walker, ed. M. Katz, (Plenum Press, New York) 1961.
26. W.D.Machin; Can.J.Chem. 1967, 45, 1904.

27. P.E. Emmett and S. Brunbauer; J.Am.Chem.Soc., 1937,59, 1563.
28. Thermodynamics for Chemists; S. Glasstaur, (D.van Nostrand, New York, 1958).
29. E.V.Ballow and S.Ross; J.Phys.Chem.1953,57,653.
30. G.J.Young et al; J.Phys.Chem. 1954, 58,313.
31. L.E.Drain and J.L.Morrison; Trans.Far.Soc. 1952,48,840; 1953, 49, 654.
32. J.R.Sams, G. Constabaris, G.D.Halsey; J.Phys. Chem. 1962,66,2154.
33. The Adsorption of Gases and Vapours; S.Brunnever, (University Press, Princeton) 1943.
34. J.Holmes, R.Beebe; Can.J.Chem. 1957,35,1542.
35. A. Textbook of Physical Chemistry, S. Glasstone; (Van Nostrand, New York) 1957.
36. Molecular Theory of Liquids, Herschfelder, Curtis and Reid (J. Wiley, New York) 1967.
37. Lange Handbook of Chemistry; (McGraw Hill) 1961.
38. R.C. Tolman; J.Chem.Phys. 1949,17,333.
39. C.Pierce; J.Phys.Chem. 1968, 72,3673.  
C. Pierce, J.Phys.Chem. 1959,63,1076.
40. J.W.S.Jamieson et al; Can.J.Chem. 1965,43,2148,  
J.W.S.Jamieson et al; Can.J.Chem. 1965,43,3129,  
G.B.Frost,K.A.Moon and E.H.Tompkins; Can.J.Chem. 1951,29,604.
41. P.Tarkington; Trans. Far.Soc. 1950,46,894.

42. U.S. Dept. of Commerce; Selected Values of  
Chemical Thermodynamic Properties, Circular 500,  
Pt. 1, 1952. National Bureau of Standards.

CALIBRATION OF THE SPOON GAUGE

The spoon gauge was calibrated against an oil manometer (Octoil S CVC Lot BL 19) for pressure up to 11 mm of mercury, and against the mercury manometer in the pressure range between 11 and 15 mm of mercury. The oil was degassed before use. The specific gravities of the oil were measured at different temperatures with a Westphal Balance and are listed in Table 1 and are plotted in Figure 1. Values for the density of mercury at various temperatures were taken from the Handbook of Chemistry and Physics (24) and are summarized in Table 1. The values of the ratio of the density of oil to the density of mercury are shown in Figure 2.

TABLE 1DENSITIES OF OIL AND MERCURY AT VARIOUS TEMPERATURESAND THE RATIOS OF THESE DENSITIES

Temperature °C	Density		
	Oil gm cm <sup>-3</sup>	Mercury gm cm <sup>-3</sup>	Ratio $\frac{\rho_{\text{oil}}}{\rho_{\text{H}_3}}$
25.6°	0.9085	13.5325	14.8954
26.8	0.9077	13.5296	14.9053
31.6	0.9039	13.5178	14.9549
36.7	0.8998	13.5053	15.0092

The levels of the oil columns were measured with a cathetometer sensitive to  $\pm 0.005$  mm. After each pressure change, the system was allowed to equilibrate for at least 20 minutes or until no change in the oil column levels could be observed. Each measurement was repeated three times and the average was used. The pressure could be read to an accuracy corresponding to  $\pm 0.007$  mm of mercury.

The resistances were read to  $\pm 0.05 \Omega$  which corresponds to ca.  $\pm 0.0025$  mm of mercury. To compensate for the drift in the system, the zero point was checked periodically during runs.

Values of resistances and corresponding pressure are listed in Table 2 of this Appendix, and are plotted in Figure 3.

TABLE 2CALIBRATION DATA FOR SPOON GUAGE WITH AIR

<u>Run 1</u>	Pressure		Resistance
mm oil	mm mercury		( $\Omega$ )
0.49	0.0329		0.7
1.15	0.0771		2.1
2.10	0.1408		3.9
2.98	0.1998		5.8
6.70	0.4492		13.4
4.77	0.3199		9.4
6.59	0.4419		13.1
23.25	1.5591		48.6
18.96	1.2715		39.3
16.85	1.1298		34.7
14.57	0.9769		29.8
11.27	0.7556		22.6
12.99	0.8712		26.2
15.34	1.0283		15.34
23.37	1.5663		48.5
21.26	1.4248		44.0
18.46	1.2372		38.5
16.20	1.0856		33.4

TABLE 2 (CONT'D)

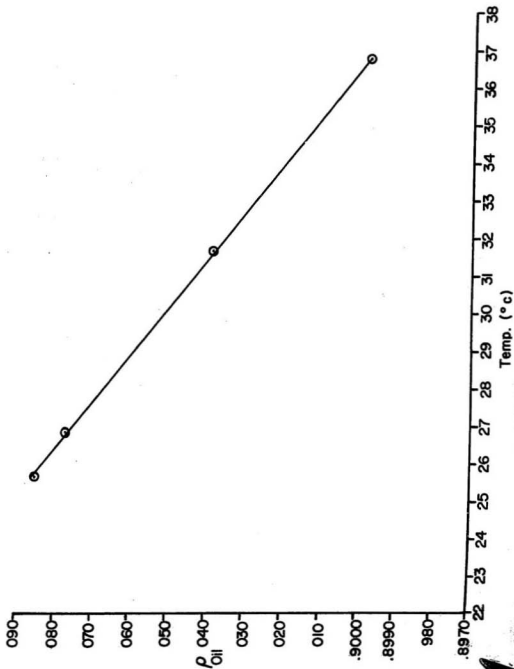
<u>Run 2</u>	Pressure	Resistance
mm oil	mm mercury	( $\Omega$ )
2.05	0.1374	3.85
6.45	0.4323	12.8
15.73	1.0544	32.2
18.68	1.2493	38.2
24.08	1.613	50.0
33.98	2.277	72.6
41.26	2.764	88.9
47.14	3.158	102.7
57.35	3.843	127.6
53.89	3.613	119.0
60.55	4.060	135.6
72.05	4.8307	165.4
92.97	6.233	222.1
106.99	7.173	263.2
118.74	7.960	299.5
137.18	9.195	360.7
149.85	10.063	409.7
148.94	10.002	405.0
146.72	9.853	397.4
134.98	9.062	356.0
131.55	8.831	344.5
122.16	8.201	312.6

TABLE 2 (CONT'D)

Pressure		Resistance
mm oil	mm mercury	( $\Omega$ )
118.29	7.941	300.3
108.64	7.293	270.1
102.84	6.900	252.3
90.51	6.072	216.0
81.35	5.457	190.4
84.26	5.659	199.3
77.95	5.235	182.1
74.21	4.984	172.3
78.84	5.286	183.4
71.64	4.804	164.3
68.57	4.598	156.0
63.89	4.285	143.3
58.12	3.897	129.7
50.43	3.381	110.8
41.45	2.779	89.7
38.52	2.588	83.0
31.98	2.144	68.0
30.74	2.0614	62.9
25.03	1.6783	52.2
22.76	1.526	47.41
18.11	1.214	37.3
15.38	1.031	31.6
8.84	5.927	17.6
6.88	0.4613	13.7

TABLE 2 (CONT'D)

mm oil	Pressure	mm mercury	Resistance ( $\Omega$ )
5.52		0.3699	11.0
3.99		0.2674	7.7
1.82		0.12196	3.2
1.27		0.08511	2.0
0.80		0.05361	1.0

Density of oil vs. temperature.

Ratio  $\frac{\rho_{oil}}{\rho_{Hg}}$  at Various Temperatures.

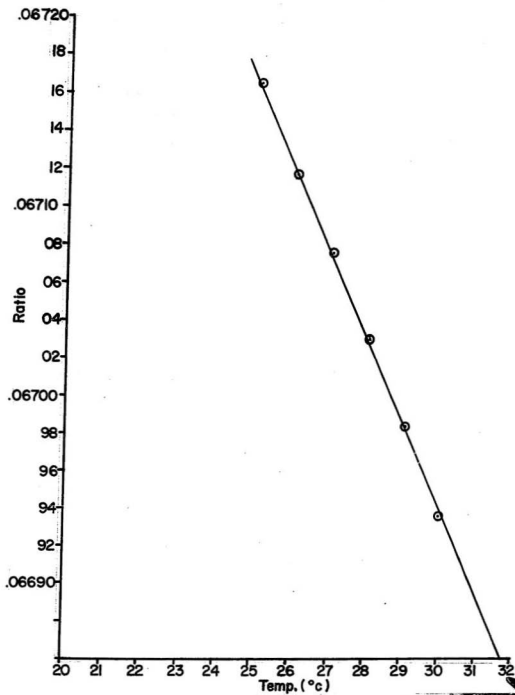


FIGURE-3

Appendix - I

Calibration curve of spoon gauge.

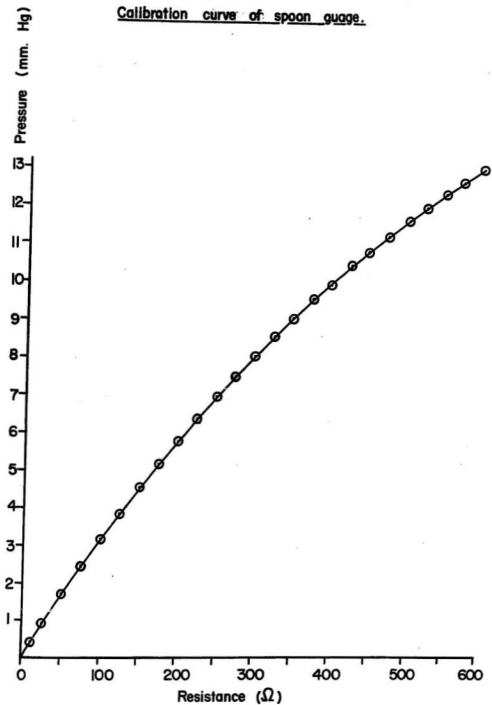


TABLE 1

DATA FOR BALANCE CALIBRATION WITH  
TRICHLOROFLUOROMETHANE AND  
BUOYANCY BULB AT 20° C

<u>Run 1</u>		<u>Run 2</u>	
Pressure (cm of Hg)	EMF* (volts)	Pressure (cm of Hg)	EMF* (volts)
0	0.3000	0	0.3021
0.133	0.2979	2.667	0.2738
0.298	0.2962	4.273	0.2475
0.516	0.2940	8.63	0.2141
1.393	0.2851	11.544	0.1844
3.459	0.2641	14.841	0.1504
5.319	0.2456	18.141	0.1163
9.432	0.2031	21.439	0.0825
10.407	0.1932	-	-
15.873	0.1371	18.540	0.1131
18.356	0.1111	16.209	0.1369
21.517	0.0788	12.440	0.1756
23.061	0.0636	9.480	0.2061
-	-	6.319	0.2384
17.588	0.0981	3.141	0.2712
17.424	0.1215	1.406	0.2880
14.237	0.1544	0.101	0.3016
10.304	0.1948		
6.627	0.2325		

TABLE 1 (CONT'D)Run 1

Pressure (cm of Hg)	EMF* (volts)
3.033	0.2693
1.797	0.2820

\*across standard resistance

TABLE 2

DATA FOR BALANCE CALIBRATION WITH  
TRICHLOROFLUOROMETHANE AND GLASS BEAD AT 20°C

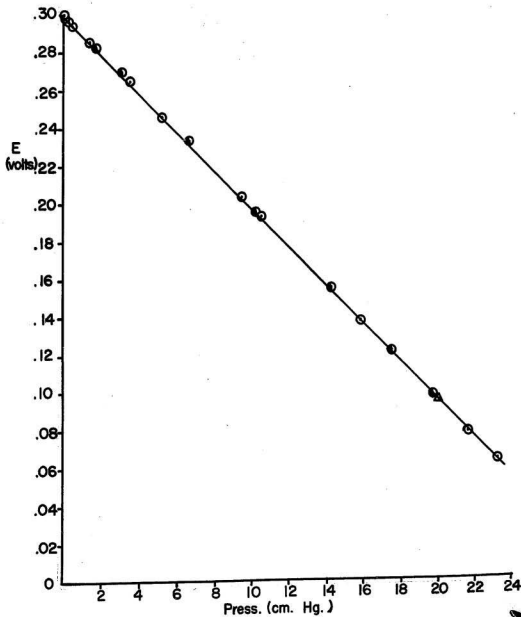
<u>Run 1</u>		<u>Run 2</u>	
Pressure (cm Hg)	EMF* (volts)	Pressure (cm Hg)	EMF* (volts)
8.554	0.0806	16.589	0.0814
11.720	0.0807	9.971	0.0815
8.073	0.0807	5.302	0.0815
2.777	0.0810	3.800	0.0816
1.296	0.0810	1.629	0.0815
0.485	0.0808	0.000	0.0815
0.000	0.0808		

\*across standard resistance

Balance calibration with Trichlorofluoromethane  
and buoyancy bulb at 20°. (Run 1).

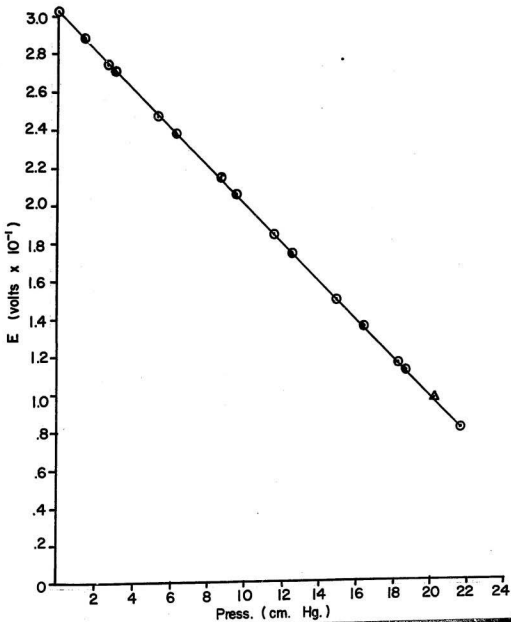
Int. = .29969 v

Slope =  $-1.0247 \times 10^{-2}$  v/cm.



Balance calibration with Trichlorofluoromethane  
and buoyancy bulb at 20°c. (Run 2).

Slope =  $-1.02305 \times 10^{-2}$  v/cm.  
Int. = .3024 v



Balance calibration with Trichlorofluoromethane  
and glass bead at 20° c. (Run 1).

Balance Calibration (p.79)

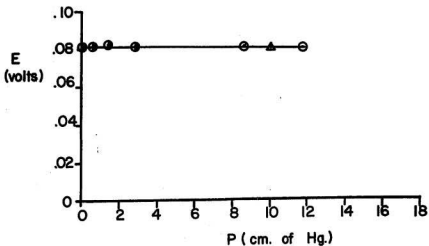
Fron II

20.0° c

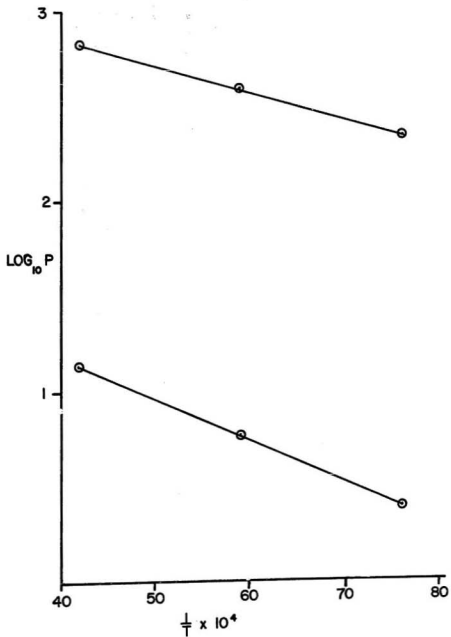
Glass bead

Slope =  $-0.0022 \times 10^{-2}$  v/cm

Int. = .0809



Measured values of the  $\log_{10}$  vapour pressures of  
Tetrachloroethylene and Trichlorofluoritethane vs.  $\frac{1}{T}$ .



TABULATION OF SORPTION DATA

## I. Trichlorofluoromethane Sorption Data.

## A. Data at 20°C.

Run 1

Pressure (torr)	Weight Adsorbed ( $\mu$ moles)
12.15	4.92:
54.01	16.38
108.50	26.83
153.79	33.82
204.09	40.59
248.42	46.34
298.73	54.75
387.45	67.12
458.0	81.43
538.00	118.68
666.00	535.09
485.84	125.56
384.86	84.19
302.06	60.99
247.52	44.90
200.14	39.20
144.19	31.55
99.13	25.04
56.16	17.33

Run 1 (cont'd)

Pressure (torr)	Weight Adsorbed ( $\mu$ moles)
16.79	8.20
0.0	0.0

Run 2

48.97	13.44
95.89	22.54
200.21	37.25
301.62	49.36
396.30	62.63
500.05	90.61
607.0	222.53
483.97	109.01
393.99	80.94
296.74	53.68
193.35	37.45
99.32	24.41
47.15	14.33
3.6	1.03

Run 3

50.00	15.23
100.05	24.58
150.07	32.04
203.01	38.80
276.27	47.58
378.74	60.91
493.42	84.22
506.39	95.35
544.0	117.70
552.0	127.37
569.0	145.88
591.0	182.29
613.0	264.18
631.0	410.34
666.0	off scale
616.0	381.24
595.0	270.08
561.0	186.75
541.0	162.20
482.20	116.89
416.46	91.68
363.40	78.46
316.71	68.79
294.24	52.19
279.89	48.04

Run 3 (cont'd)

Pressure (torr)	Weight Adsorbed ( $\mu$ moles)
265.09	45.85
219.10	40.10
154.20	31.89
103.14	24.55
59.02	16.41
0.00	0.0

B. Data at 5.8<sup>o</sup>C.

Pressure (torr)	Weight Adsorbed ( $\mu$ moles)
17.19	11.37
29.10	16.49
43.50	21.90
59.82	26.80
86.60	33.42
101.40	36.84
115.07	39.43
130.85	42.63
146.50	45.77
154.95	48.16
164.95	48.16
169.23	50.23
187.32	53.85
203.32	57.71
218.50	61.63

## B. Data at 5.8°C (cont'd)

Pressure (torr)	Weight Adsorbed ( $\mu$ moles)
232.92	65.97
252.91	73.57
266.64	80.65
282.40	89.69
299.64	105.12
326.64	126.94
329.15	152.41
339.89	183.12
355.19	277.79
369.21	482.42
384.83	552.25
351.25	351.71
318.85	181.97
299.37	148.12
280.60	127.66
263.24	113.44
245.61	100.05
225.53	89.32
206.52	80.94
188.25	73.57
167.49	67.01
148.92	50.94
137.92	45.05
114.62	39.35
98.32	35.98
50.50	23.78
0.0	0

C. Data at  $-7.45^{\circ}\text{C}$ .

Pressure (torr)	Weight Adsorbed ( $\mu$ moles)
6.81	8.7791
9.03	10.8803
12.18	13.9602
16.97	17.8172
23.29	22.2788
31.28	26.9993
39.40	30.8276
48.67	34.8862
55.84	37.9373
63.49	40.8444
72.02	44.0682
79.27	45.9104
89.77	49.5084
100.20	53.2216
118.81	61.0220
139.15	73.0537
154.22	87.4457
174.36	122.5910
189.96	187.2398
201.76	323.4457
180.93	200.97
164.06	145.27
133.03	100.11
118.68	87.13

C. Data at  $-7.45^{\circ}\text{C}$  (cont'd)

Pressure (torr)	Weight Adsorbed ( $\mu$ moles)
95.56	71.41
86.07	65.94
71.06	48.36
64.12	41.68
59.01	39.49
50.87	35.49
43.63	32.50
36.79	29.99
33.07	27.17
28.76	24.84
25.46	23.06
22.85	21.36
17.49	17.85
12.63	13.91
9.76	11.31
6.27	7.95
4.60	6.05
3.81	4.26
0	0

## II. TETRACHLOROETHYLENE SORPTION DATA

Data at 20°C.

Run 1

Pressure (torr)	Weight Adsorbed ( $\mu$ moles)
0.38	2.46
0.42	3.70
0.77	7.37
1.04	10.85
2.19	23.53
2.69	29.21
3.11	32.78
4.19	41.13
5.21	48.71
5.94	53.91
7.26	65.16
7.96	72.24
9.75	104.27
12.31	228.80
8.17	102.48
6.39	80.83
3.06	48.76
2.67	44.54
2.34	40.27
1.97	25.70
0.55	6.80

## II.

## A. (cont'd)

Run 2

Pressure (torr)	Weight Adsorbed ( $\mu$ moles)
0.04	0.64
0.11	1.74
0.34	4.67
0.54	6.94
0.99	13.26
2.73	31.12
3.69	38.55
5.21	49.20
7.27	65.83
9.34	94.35
10.28	124.10
10.40	127.94
11.23	166.76
11.98	176.49
11.39	187.10
11.20	179.30
10.39	150.83
9.57	126.15
7.82	99.04
5.29	71.70
2.85	49.26
2.69	47.50

## II.

## A. (cont'd)

Run 2 (cont'd)

Pressure (torr)	Weight Adsorbed ( $\mu$ moles)
2.28	42.80
1.95	30.07

Run 3

Pressure (torr)	Weight Adsorbed ( $\mu$ moles)
0.05	0.76
0.08	1.36
0.12	1.93
0.19	2.93
0.27	3.89
0.51	6.87
0.68	8.92
0.84	10.78
1.00	12.49
1.18	14.64
1.24	16.26
1.65	20.03
2.00	23.65
2.38	27.71

## II.

## A. (Cont'd)

Run 3 (cont'd)

Pressure (torr)	Weight Adsorbed ( $\mu$ moles)
2.55	29.16
3.15	34.41
3.69	38.45
4.45	43.99
5.11	48.52
5.77	53.36
6.26	57.27
6.91	62.56
7.45	67.52
7.94	72.74
8.45	79.16
8.94	87.08
9.40	95.44
9.85	105.98
10.17	120.07
10.67	138.05
11.23	167.83
11.40	179.23
11.49	185.17
11.53	190.27
11.67	200.00
11.73	207.15
11.76	211.54

## II.

## A (Cont'd)

Run 3 (cont'd)

Pressure (torr)	Weight Adsorbed ( $\mu$ moles)
11.88	217.88
11.94	224.27
2.13	24.44
2.53	28.47
5.06	47.45
7.68	69.41
10.48	130.57
11.86	227.11
12.66	339.2511
11.96	293.99
11.54	253.57
10.06	158.22
8.48	114.35
3.65	57.96
2.50	45.37
2.41	44.04
2.33	43.18
2.24	40.13
2.16	35.05
2.04	29.61
1.95	27.11
1.75	24.56
1.03	14.31

## A. (Cont'd)

Run 4

Pressure (torr)	Weight Adsorbed ( $\mu$ moles)
11.60	203.36
10.55	151.45
9.95	132.73
9.32	116.81
8.62	104.17
9.32	110.99
10.07	120.98
10.6	135.10

Run 5

11.97	251.88
11.48	217.59
11.00	187.96
10.48	167.76
9.91	140.65
9.28	125.62
8.67	113.23
7.89	103.53
6.89	88.05

## A. (Cont'd)

Run 6

Pressure (torr)	Weight Adsorbed ( $\mu$ moles)
12.44	337.67
12.05	282.21
11.47	232.47
10.86	191.25
10.14	155.93
9.32	127.06
8.43	109.20

Run 7

12.14	303.02
11.85	268.86
11.48	233.40
10.99	197.90
10.50	173.72
9.87	140.70
9.17	122.36
8.22	105.05

## B. Data at 5.8°C.

Run 1

0.35	9.94
0.85	22.56
1.29	31.54
2.33	48.07
3.22	65.95

## B. (Cont'd)

Run 1 (Cont'd)

Pressure (torr)	Weight Adsorbed ( $\mu$ moles)
3.71	79.76
4.38	113.75
5.55	403.31
5.44	409.20

Run 2

0.05	1.29
0.29	7.51
0.68	17.55
0.97	24.22
1.30	31.26
1.60	36.00
2.04	43.06
2.60	51.98
3.07	61.30
3.61	75.61
4.20	94.01
4.53	122.03
4.93	167.36
5.06	188.98

Run 3

3.54	73.56
4.70	133.07
5.19	226.03

Run 3 (cont'd).

Pressure (torr)	Weight Adsorbed ( $\mu$ moles)
5.48	322.10
5.57	350.59
5.60	383.28

Run 4

3.69	73.58
4.60	123.32
5.13	199.83
5.28	246.54
5.50	344.27
5.27	321.45
1.39	47.33
1.25	44.04
1.01	37.84
0.82	32.98
0.70	24.73
0.53	15.66
0.37	10.13
0.27	8.00

Run 5

Pressure (torr)	Weight Adsorbed ( $\mu$ moles)
6.00	205.70
4.57	174.77
4.39	148.04
4.15	134.52
3.87	119.50
3.67	109.82
3.37	98.75
3.07	88.60
2.78	79.83
2.49	72.42
2.22	65.71
1.87	57.94
1.62	51.58
1.29	43.85
0.99	36.05
0.74	33.91
0.34	7.58

Run 6

5.31	372.50
3.08	88.62
0.68	19.34
0.62	16.40

C. Data at  $-7.45^{\circ}$  C.Run 1

Pressure (torr)	Weight Adsorbed ( $\mu$ moles)
0.06	3.65
0.11	6.44
0.27	15.02
0.36	20.84
0.44	25.54
0.55	29.42
0.77	37.48
0.99	45.71
2.34	414.87
2.22	394.82
2.19	363.20
2.17	327.99
2.07	280.80
1.98	216.07
1.77	151.57
1.61	126.94
1.45	109.54
1.22	89.24
0.99	74.32
0.85	66.36
0.73	59.46
0.64	54.68
0.48	44.54
0.43	41.32
0.34	36.07

C. (Cont'd)

Run 1 (cont'd)

Pressure (torr)	Weight Adsorbed ( $\mu$ moles)
0.22	27.56
0.18	17.19
0.15	12.54

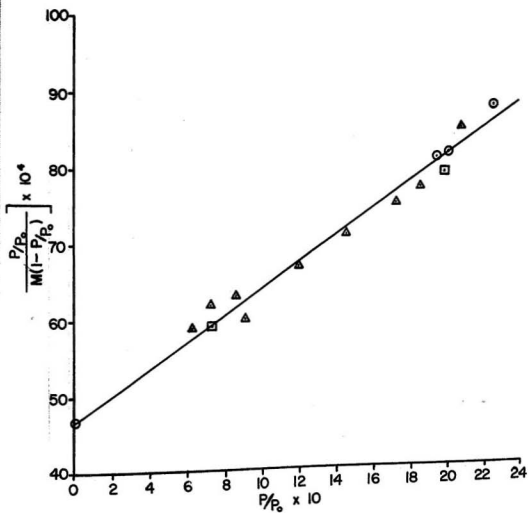
Run 2

0.06	3.39
0.34	18.91
0.46	24.75
0.69	33.95
0.99	45.44
1.16	52.53
1.31	59.56
1.54	74.49
1.67	87.15
1.81	106.77
1.93	129.44
2.04	162.10
2.11	194.42
2.21	254.12
2.55	429.18
2.23	411.39
2.11	295.37
1.94	204.88

C. (Cont'd)

Run 2 (cont'd)

Pressure (torr)	Weight Adsorbed ( $\mu$ moles)
1.68	142.32
1.46	113.59
0.91	71.84
0.42	41.49
0.34	36.24
0.31	35.00
0.28	32.24
0.24	29.97
0.23	28.23
0.21	25.18
0.18	21.01
0.16	15.50
0.13	12.33

BET Plot for Tetrachloroethylene at 20°C.

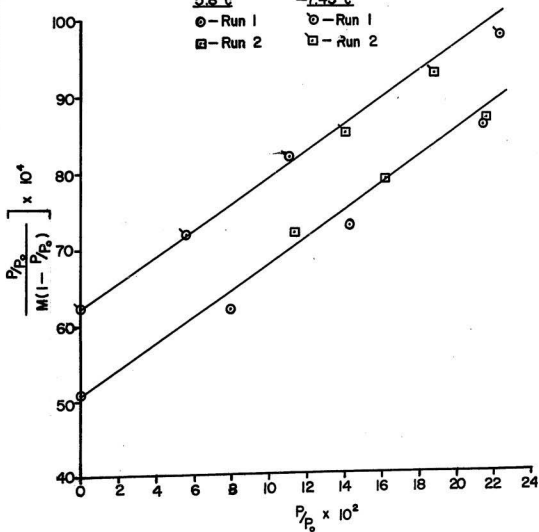
BET Plot for Tetrachloroethylene at 5.8°C and -7.45°C.Legend5.8°C-7.45°C

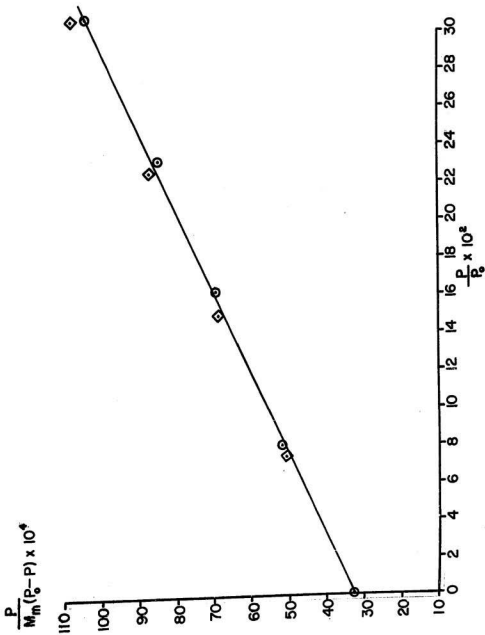
⊙ - Run 1

⊙ - Run 1

⊠ - Run 2

⊠ - Run 2



BET Plot for Trichlorofluoromethane at 20°C.

BET Plots for Trichlorofluoromethane at 5.8°C and -7.45°C.

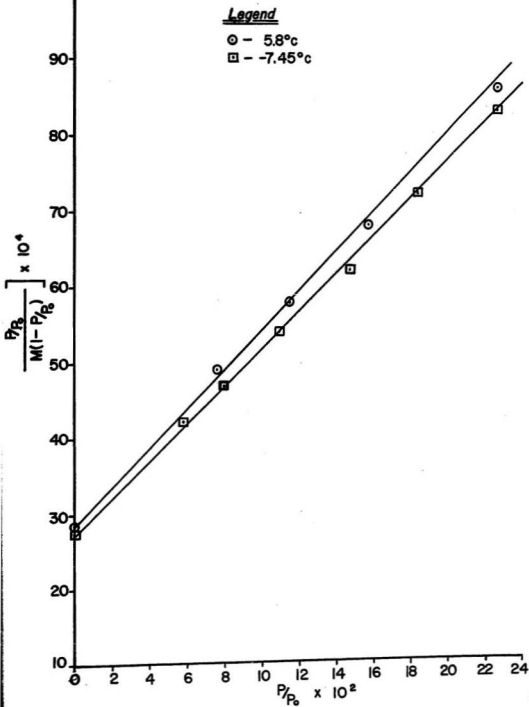


TABLE 1

ISOSTERIC AND DIFFERENTIAL HEATS OF ADSORPTIONI. TETRACHLOROETHYLENE - ADSORPTION

Quantity Adsorbed ( $\mu$ moles)	Isosteric (K cal mol <sup>-1</sup> )	Heats		
		20.0°C 8.2376	5.8°C 8.2657	-7.45°C 8.2921
5.0000	8.8201	8.2620	8.2902	8.3166
10.0000	8.8445	8.2198	8.2479	8.2744
15.0000	8.8023	8.1384	8.1666	8.1930
20.0000	8.7210	8.1243	8.1524	8.1789
22.1000	8.7068	8.0733	8.1014	8.1279
25.0000	8.6558	8.0832	8.1113	8.1377
30.0000	8.6657	8.0189	8.0470	8.0734
35.0000	8.6014	8.0462	8.0743	8.1008
40.0000	8.6287	8.1386	8.1668	8.1932
44.1000	8.7211	8.3554	8.3835	8.4099
50.0000	8.9379	8.4753	8.5034	8.5298
55.0000	9.0578	8.5961	8.6242	8.6507
60.0000	9.1786	8.6602	8.6883	8.7147
66.2000	9.2427	8.7212	8.7493	8.7758
70.0000	9.3037	8.7726	8.8007	8.8271
75.0000	9.3551	8.8142	8.8424	8.8688
80.0000	9.3967	8.8593	8.8875	8.9139
85.0000	9.4418	8.8822	8.9104	8.9368
88.2000	9.4647	8.8992	8.9274	8.9538
90.0000	9.4817			

TABLE 1 (CONT'D)

I. Cont'd.	Isosteric (K cal mol <sup>-1</sup> )	Heats		
		20.0°C	5.8°C	-7.45°C
Quantity Adsorbed ( $\mu$ moles) 100.0000	9.5095	8.9270	8.9551	8.9815
110.0000	9.5127	8.9302	8.9583	8.9847
105.0000	9.5011	8.9186	8.9467	8.9732
115.0000	9.5101	8.9276	8.9557	8.9821
120.0000	9.5134	8.9309	8.9590	8.9854
125.0000	9.4932	8.9107	8.9388	8.9652
130.0000	9.5126	8.9301	8.9582	8.9846
132.3000	9.5206	8.9381	8.9662	8.9926
140.0000	9.5742	8.9917	9.0198	9.0462
145.0000	9.5908	9.0083	9.0364	9.0629
150.0000	9.6050	9.0225	9.0506	9.0770
154.4000	9.6136	9.0311	9.0592	9.0857
160.0000	9.6209	9.0384	9.0665	9.0929
165.0000	9.6222	9.0397	9.0679	9.0943
170.0000	9.6278	9.0453	9.0734	9.0998
176.4000	9.6363	9.0538	9.0819	9.1083
180.0000	9.6306	9.0481	9.0762	9.1026
185.0000	9.6377	9.0551	9.0833	9.1097
190.0000	9.6376	9.0551	9.0832	9.1097
198.5000	9.6202	9.0377	9.0658	9.0923
205.0000	9.6189	9.0364	9.0645	9.0909
210.0000	9.6213	9.0388	9.0669	9.0934

TABLE 2

## II. TETRACHLOROETHYLENE - DESORPTION+

Quant. Ads. ( $\mu$ moles)	Isosteric*	Differential*		
		20.0°C	5.8°C	-7.45°C
45.0000	9.3968	8.8143	8.8424	8.8688
50.8000	9.3859	8.8033	8.8315	8.8579
55.0000	9.5008	8.9183	8.9464	8.9728
60.0000	9.5860	9.0035	9.0316	9.0580
65.0000	9.6900	9.1074	9.1356	9.1620
70.0000	9.7266	9.1441	9.1723	9.1987
76.2000	9.8642	9.2817	9.3099	9.3363
80.0000	9.8081	9.2256	9.2538	9.2802
85.0000	9.8401	9.2576	9.2858	9.3122
90.0000	9.8350	9.2525	9.2806	9.3071
95.0000	9.8195	9.2370	9.2651	9.2915
101.6000	9.9466	9.3641	9.3923	9.4187
105.0000	9.8314	9.2489	9.2770	9.3034
110.0000	9.8204	9.2379	9.2661	9.2925
115.0000	9.7798	9.1973	9.2254	9.2519
120.0000	9.7617	9.1792	9.2073	9.2337
127.0000	9.7366	9.1541	9.1823	9.2087
130.0000	9.7634	9.1809	9.2091	9.2355
135.0000	9.7866	9.2041	9.2322	9.2587
140.0000	9.7452	9.1627	9.1909	9.2173
145.0000	9.7678	9.1853	9.2134	9.2399
160.0000	9.7848	9.2023	9.2304	9.2568
165.0000	9.7385	9.1560	9.1841	9.2106

\* (K cal mol<sup>-1</sup>)

TABLE 2 (CONT'D)

II. (Cont'd) Quant. Ads. ( $\mu$ moles)	Isosteric*	Differential*		
		20.0°C	5.8°C	-7.45°C
170.0000	9.7957	9.2132	9.2413	9.2678
177.8000	9.7363	9.1538	9.1819	9.2083
180.0000	9.7220	9.1395	9.1676	9.1941
185.0000	9.7154	9.1329	9.1611	9.1875
190.0000	9.7207	9.1381	9.1663	9.1927
195.0000	9.7229	9.1404	9.1685	9.1950
200.0000	9.7222	9.1397	9.1678	9.1942
203.2000	9.7303	9.1478	9.1759	9.2024
210.0000	9.7153	9.1328	9.1610	9.1874
215.0000	9.7162	9.1336	9.1618	9.1882
220.0000	9.7100	9.1275	9.1557	9.1821
228.6000	9.7110	9.1285	9.1566	9.1831
230.0000	9.7166	9.1340	9.1622	9.1886
235.0000	9.7160	9.1335	9.1617	9.1881
240.0000	9.7100	9.1275	9.1556	9.1820
245.0000	9.7177	9.1352	9.1634	9.1898
250.0000	9.7193	9.1367	9.1649	9.1913
254.0000	10.3411	9.7586	9.7867	9.8131

\*(K cal mol<sup>-1</sup>)

TABLE 3

## III. TRICHLOROFLUOROMETHANE - ADSORPTION

Quant. Ads. ( $\mu$ moles)	Isosteric*	Differential*		
		20.0°C	5.8°C	-7.45°C
5.0000	7.2158	6.6333	6.6614	6.6878
10.0000	7.1756	6.5930	6.6212	6.6476
15.0000	9.4210	8.8385	8.8666	8.8930
18.0000	7.3417	6.7592	6.7873	6.8137
20.0000	7.2535	6.6710	6.6992	6.7256
25.0000	7.3259	6.7434	6.7715	6.7980
30.0000	7.2328	6.6502	6.6784	6.7048
35.9000	6.9052	6.3227	6.3508	6.3772
40.0000	6.9675	6.3850	6.4131	6.4396
45.0000	6.9494	6.3669	6.3950	6.4214
50.0000	6.8185	6.2360	6.2641	6.2906
53.9000	6.7972	6.2147	6.2428	6.2693
60.0000	6.7663	6.1838	6.2119	6.2384
65.0000	6.7357	6.1532	6.1813	6.2078
70.0000	6.6496	6.0671	6.0952	6.1217
71.8000	6.6613	6.0788	6.1070	6.1334
75.0000	6.6010	6.0185	6.0466	6.0731
80.0000	6.5753	5.9928	6.0210	6.0474
85.0000	6.5446	5.9621	5.9903	6.0167
89.8000	6.4869	5.9044	5.9235	5.9589

\* (K cal mol<sup>-1</sup>)

## III. (cont'd)

Quant. Ads. ( $\mu$ moles)	Isosteric*	Differential*		
		20.0°C	5.8°C	-7.45°C
95.0000	6.4983	5.9158	5.9439	5.9703
100.0000	6.4957	5.9132	5.9413	5.9678
105.0000	6.4717	5.8892	5.9174	5.9438
107.7000	6.4782	5.8957	5.9239	5.9503
115.0000	6.4614	5.8791	5.9072	5.9337
120.0000	6.4603	5.8778	5.9060	5.9324
125.7000	6.4591	5.8765	5.9047	5.9311
130.0000	6.3828	5.8002	5.8284	5.8548
135.0000	6.4504	5.8679	5.8961	5.9225
140.0000	6.4495	5.8670	5.8951	5.9215
143.6000	6.4896	5.9071	5.9353	5.9617
150.0000	6.4547	5.8722	5.9003	5.9267
155.0000	6.4538	5.8713	5.8995	5.9259
161.6000	6.4463	5.8638	5.8919	5.9183
170.0000	6.4584	5.8759	5.9040	5.9305
175.0000	6.4643	5.8818	5.9099	5.9363
185.0000	6.4505	5.8680	5.8962	5.9226
190.0000	6.4564	5.8739	5.9020	5.9284
200.0000	6.4432	5.8607	5.8888	5.9152

\* (K cal mol<sup>-1</sup>)

TABLE 4

IV. TRICHLOROFLUOROMETHANE - DESORPTION

Quant. Ads. ( $\mu$ moles)	Isosteric*	Differential*		
		20.0°C	5.8°C	-7.45°C
50.0000	1.5470	0.9645	0.9927	1.0191
53.9000	7.9975	7.4150	7.4431	7.4696
55.0000	7.9083	7.3258	7.3539	7.3804
60.0000	7.6793	7.0968	7.1249	7.1513
65.0000	7.4664	6.8839	6.9120	6.9384
70.0000	7.3256	6.7431	6.7712	6.7976
71.8000	7.2665	6.6840	6.7122	6.7386
75.0000	7.1818	6.5993	6.6274	6.6539
80.0000	7.0854	6.5029	6.5310	6.5574
85.0000	6.9382	6.3557	6.3838	6.4103
89.8000	6.9900	6.4075	6.4356	6.4620
95.0000	6.9502	6.3677	6.3959	6.4223
100.0000	6.9178	6.3353	6.3635	6.3899
105.0000	6.8749	6.2924	6.3205	6.3469
107.7000	6.8501	6.2676	6.2957	6.3221
115.0000	6.7658	6.1833	6.2114	6.2378
120.0000	6.7057	6.1232	6.1513	6.1777
125.0000	6.6708	6.0883	6.1164	6.1429
125.7000	6.6700	6.0875	6.1156	6.1420
130.0000	6.6499	6.0674	6.0956	6.1220
135.0000	6.6223	6.0398	6.0680	6.0944

\* (K cal mol<sup>-1</sup>)

TABLE 4 (Cont'd)

IV. (Cont'd)		Differential*		
Quant. Ads. ( $\mu$ moles)	Isosteric*	20.0°C	5.8°C	-7.45°C
	140.0000	6.6032	6.0207	6.0489
143.6000	6.5933	6.0108	6.0390	6.0654
145.0000	6.5778	5.9953	6.0234	6.0498
150.0000	6.5603	5.9778	6.0059	6.0234
155.0000	6.5573	5.9748	6.0029	6.0294
160.0000	6.5480	5.9655	5.9937	6.0201
161.6000	6.5473	5.9648	5.9929	6.0194
165.0000	6.5477	5.9652	5.9934	6.0198
170.0000	6.5300	5.9475	5.9757	6.0021
175.0000	6.5282	5.9457	5.9738	6.0003
179.5000	6.5201	5.9376	5.9658	5.9922
185.0000	6.5186	5.9361	5.9643	5.9907
190.0000	6.5174	5.9348	5.9630	5.9894
200.0000	6.5018	5.9193	5.9474	5.9738

\* (K cal mol<sup>-1</sup>)

STANDARD ENTROPIES, HEAT CAPACITIES OF ADSORBATES

[Source indicated in square bracket]

<u>Property</u>	<u>Tetrachloroethylene</u>	<u>Trichlorofluoromethane</u>
$S_G(120^\circ\text{C}) +$	89.4 cal deg <sup>-1</sup> mole <sup>-1</sup> [41]	74.06 cal deg <sup>-1</sup> mole <sup>-1</sup> [42] (25°C)
$S_{G-L}(120^\circ\text{C})$	21.0 cal deg <sup>-1</sup> mole <sup>-1</sup> [42]	20.1 cal deg <sup>-1</sup> mole <sup>-1</sup> [42] (at 23.6°C)
$C_p(\text{liquid})$	35.8 cal deg <sup>-1</sup> mole <sup>-1</sup> [42]	29.05 cal deg <sup>-1</sup> mole <sup>-1</sup> [42]
$C_p(\text{gas})$	-	18.73 cal deg <sup>-1</sup> mole <sup>-1</sup> [42]

THEORETICAL ENTROPY CHANGE FOR  
TRANSITION FROM GAS TO LIQUID FOR  
TETRACHLOROETHYLENE AND TRICHLOROFLUOROMETHANE

Coverage ( $\mu$ moles)	<u>Tetrachloroethylene</u>		<u>Trichlorofluoromethane</u>	
	$S_{\text{Gas}}^*$	$S_{\text{G}}^* - S_{\text{L}}^*$	$S_{\text{Gas}}^*$	$S_{\text{G}}^* - S_{\text{L}}^*$
5	97.3	39.4	81.68	27.27
10	95.8	37.9	80.21	26.80
15	94.9	37.0	79.18	26.77
20	94.3	36.4	78.70	25.29
22.1	94.1	36.2	-	-
25.0	96.8	35.9	78.42	25.01
30.0	93.4	35.4	77.76	24.35
35.0	93.0	35.1	77.20	23.79
40.0	92.6	34.7	76.64	23.23
44.1	92.3	34.4	-	-
50.0	92.0	34.1	75.53	22.12
60.0	91.6	33.7	75.34	21.93
66.2	91.4	33.5	-	-
70.0	91.3	33.4	74.95	21.54
75.0	91.1	33.2	74.84	21.43
80.0	91.1	33.2	74.80	21.39
85.0	91.0	33.1	74.75	21.34
88.2	90.9	33.0	-	-
90.0	90.9	33.0	-	-
100.0	90.8	32.9	74.58	21.17

\* cal deg<sup>-1</sup> mol<sup>-1</sup>

Coverage ( $\mu$ moles)	<u>Tetrachloroethylene</u>		<u>Trichlorofluoromethane</u>	
	$S_{\text{Gas}}^*$	$S_{\text{G}}^* - S_{\text{L}}^*$	$S_{\text{Gas}}^*$	$S_{\text{G}}^* - S_{\text{L}}^*$
105.0	90.8	33.9	74.54	21.13
110.0	90.7	32.8	-	-
115.0	90.7	32.8	74.47	21.06
120.0	90.7	32.8	74.47	27.06
125.0	90.7	32.8	-	-
130.0	90.6	32.7	74.38	20.97
132.3	90.6	32.7		
140.0	90.6	32.7	74.38	20.97
145.0	90.6	32.7	-	-
150.0	90.5	32.6	74.3	20.93
154.4	90.5	32.6	74.34	20.93
160.0	90.5	32.6	74.29	20.87
165.0	90.5	32.6	74.24	20.83
170.0	90.5	32.6	74.25	20.84
176.4	90.5	32.6	-	-
180.0	90.5	32.6	74.21	20.80
185.0	90.5	32.6	74.25	20.84
190.0	90.4	32.5	74.24	20.83
198.5	90.4	32.5		
205.0	90.4	32.5		
210.0	90.4	32.5		

\*cal deg<sup>-1</sup> mol<sup>-1</sup>

TABLE 1

TETRACHLOROETHYLENE ADSORPTION  
EXPERIMENTAL ENTROPY CHANGES ACCOMPANYING  
TRANSITION FROM GASEOUS TO ADSORBED STATE

Coverage ( $\mu$ moles)	$S'_G - \bar{S}_S^*$		
	20° C	5.8° C	-7.45° C
5.000	30.085	31.617	33.194
10.000	30.154	31.689	33.269
15.000	30.017	31.545	33.118
20.000	29.744	31.258	32.817
22.100	29.710	31.223	32.780
25.000	29.526	31.029	32.576
30.000	29.560	31.065	32.614
35.000	29.338	30.832	32.369
40.000	29.434	30.932	32.475
44.100	29.748	31.262	32.821
50.000	30.488	32.040	33.638
60.000	31.310	32.904	34.545
66.200	31.528	33.133	34.786
70.000	31.736	33.352	35.015
75.000	31.910	33.535	35.207
80.000	32.054	33.685	35.365
85.000	32.207	33.847	35.534

\* cal. deg<sup>-1</sup> mole<sup>-1</sup>

TABLE 1 (CONT'D)

Coverage ( $\mu$ moles)	$S_G' - S_S^*$		
	20° C	5.8° C	-7.45° C
88.200	32.286	33.929	35.621
90.000	32.344	33.990	35.685
100.000	32.439	34.090	35.790
105.000	32.408	34.058	35.757
110.000	32.449	34.101	35.802
115.000	32.439	34.090	35.790
120.000	32.449	34.101	35.802
125.000	32.381	34.029	35.726
130.000	32.449	34.101	35.802
132.300	32.477	34.130	35.832
140.000	32.657	34.320	36.031
145.000	32.715	34.381	36.095
150.000	32.763	34.431	36.148
154.400	32.794	34.463	36.182
160.000	32.818	34.488	36.208
165.000	32.821	34.492	36.212
170.000	32.842	34.513	36.234
176.400	32.869	34.542	36.265
180.000	32.852	34.524	36.246
185.000	32.876	34.549	36.262
190.000	32.876	34.549	36.272
198.500	32.814	34.485	36.204
205.000	32.811	34.481	36.201/
210.000	32.818	34.488	36.208

\* cal. deg<sup>-1</sup> mole<sup>-1</sup>

TABLE 2

TETRACHLOROETHYLENE DESORPTIONEXPERIMENTAL ENTROPY CHANGES ACCOMPANYINGTRANSITION FROM GASEOUS TO ADSORBED STATES.THEORETICAL ENTROPY CHANGE ACCOMPANYING LIQUEFACTION AT 20° C.

M (μ moles)	20°C	Experimental		S <sup>0*</sup> Gaseous Tetrachloro- ethylene	Theoretical
		S <sub>G</sub> <sup>0</sup> - S <sub>S</sub> <sup>0*</sup>	5.8°C		-7.45°C
50.000	32.016	33.646	35.324	94.3	34.018
55.000	32.408	34.058	35.757	94.0	33.738
60.000	32.698	34.363	36.076	93.8	33.458
65.000	33.053	34.736	36.468	93.5	33.200
70.000	33.179	34.868	36.607	93.3	32.972
76.200	33.647	35.359	37.123	93.0	32.720
80.000	33.456	35.159	36.912	92.9	32.623
85.000	33.565	35.273	37.032	92.8	32.483
90.000	33.548	35.255	37.014	92.7	32.365
95.000	33.497	35.202	36.957	92.6	32.257
101.000	33.939	35.657	37.435	92.4	32.133
105.000	33.534	35.241	36.998	92.4	32.077
110.000	33.497	35.202	36.957	92.3	32.010
115.000	33.360	35.058	36.807	92.3	31.954
120.000	33.299	34.994	36.739	92.2	31.903
127.000	33.213	34.904	36.645	92.2	31.835
130.000	33.302	34.997	36.743	92.2	31.805
135.000	33.384	35.083	36.833	92.2	31.767

\* cal deg.<sup>-1</sup> mole<sup>-1</sup>



M ( $\mu$ moles)	20°C	5.8°C	-7.45°C	Gaseous Tetrachloro- ethylene	
140.000	33.241	34.933	36.675	92.0	31.729
145.000	33.319	35.015	36.761	92.0	31.692
152.400	33.882	35.607	37.382	91.9	31.641
160.000	33.377	35.076	36.825	91.9	31.600
165.000	33.200	34.911	36.652	96.5	36.210
165.000	33.220	34.911	36.652	91.9	31.587
170.000	33.415	35.116	36.867	91.8	31.539
177.800	33.210	34.901	36.641	91.8	31.526
180.000	33.162	34.850	36.588	91.8	31.518
185.000	33.138	34.825	36.562	91.8	31.503
190.000	33.159	34.847	36.584	91.8	31.488
195.000	33.166	34.854	36.592	91.8	31.472
200.000	33.128	34.815	36.551	91.8	31.457
203.200	33.190	34.879	36.618	91.8	31.447
210.000	33.138	34.825	36.562	91.7	31.432
215.000	33.142	34.829	36.566	91.7	31.420
220.000	33.131	34.807	36.543	91.7	31.410
228.600	33.125	34.811	36.547	91.7	31.393
230.000	33.145	34.832	36.569	91.7	31.388
235.000	33.142	34.829	36.566	91.7	31.379
240.000	33.121	34.807	36.543	91.7	31.369
245.000	33.149	34.836	36.573	91.7	31.359
250.000	33.152	34.840	36.577	91.7	31.352
254.000	35.274	37.069	38.918	91.4	31.121

\* cal deg.<sup>-1</sup> mole<sup>-1</sup>

TABLE 5

TRICHLOROFLUOROMETHANE ADSORPTIONEXPERIMENTAL DIFFERENCE BETWEEN MOLAR ENTROPY OF GASEOUS STATE  
AND DIFFERENTIAL ENTROPY OF ADSORBED STATE

M ( $\mu$ moles)	$S_G' - S_S^*$			$(S_G^{20} - S_L)^*$
	20°C	5.8°C	-7.45°C	
5.000	24.614	25.867	27.157	
10.000	24.478	25.724	27.006	
15.000	32.136	33.771	35.455	
18.000	25.044	26.319	27.631	
20.000	24.744	26.003	27.300	
25.000	24.989	26.261	27.571	
30.000	24.672	25.928	27.221	
35.900	23.553	24.752	25.986	
40.000	23.768	24.978	26.224	25.68
45.000	23.703	24.910	26.152	
50.000	23.260	24.444	25.663	
53.900	23.185	24.365	25.580	
60.000	23.079	24.254	25.463	24.51
65.000	22.977	24.146	25.350	
71.800	22.721	23.877	25.068	
75.000	22.516	23.662	24.842	
80.000	22.428	23.569	24.745	

\*cal deg<sup>-1</sup> mole<sup>-1</sup>

TABLE 3 (CONT'D)

M ( $\mu$ moles)	20°C	$S_G^* - S_S^*$		$(S_G^{20} - S_L^*)^*$
		5.8°C	-7.45°C	
85.000	22.325	23.462	24.632	
89.800	22.127	23.254	24.413	
95.000	22.165	23.293	24.455	
100.000	22.158	23.286	24.447	23.91
105.000	22.076	23.200	24.357	
107.700	22.097	23.221	24.379	
115.000	22.042	23.164	24.319	
120.000	22.035	23.157	24.312	23.80
125.700	22.032	23.153	24.308	
130.000	21.773	22.881	24.022	
135.000	22.001	23.121	24.274	
140.000	22.001	23.121	24.274	
143.600	22.138	23.264	24.425	
150.000	22.018	23.139	24.293	
155.000	22.015	23.135	24.289	
161.600	21.987	23.107	24.259	
170.000	22.028	23.150	24.304	
175.000	22.049	23.171	24.327	23.64 (M=180)
185.000	22.001	23.121	24.274	
190.000	22.022	23.143	24.297	
200.000	21.977	23.096	24.248	

\* cal deg<sup>-1</sup> mol<sup>-1</sup>

TABLE 4

TRICHLOROFLUOROMETHANE - DESORPTIONEXPERIMENTAL DIFFERENCE BETWEEN MOLAR ENTROPY OF GASEOUS STATE  
AND DIFFERENTIAL ENTROPY OF ADSORBED STATE

M ( $\mu$ moles)	$S'_G - \bar{S}_S^*$		
	20°C	5.8°C	-7.45°C
50.000	5.276	5.545	5.822
53.900	27.282	28.670	30.100
55.000	26.975	28.348	29.761
60.000	26.193	27.527	28.899
65.000	25.467	26.763	28.098
70.000	24.989	26.261	27.571
71.800	24.788	26.050	27.349
75.000	24.498	25.745	27.029
80.000	24.167	25.397	26.664
85.000	23.666	24.870	26.111
89.800	23.843	25.057	26.306
95.000	23.707	24.913	26.156
100.000	23.598	24.799	26.035
105.000	23.451	24.645	25.874
107.700	23.366	24.555	25.779
115.000	23.079	24.254	25.463
120.000	22.874	24.039	25.238
125.000	22.755	23.913	25.106

\*cal deg.<sup>-1</sup> mole<sup>-1</sup>

TABLE 4 (CONT'D)

M ( $\mu$ moles)	20°C	$S_G^* - S_S^*$	
		5.8°C	-7.45°C
125.700	22.752	23.910	25.102
130.000	22.683	23.838	25.027
135.000	22.588	23.738	24.941
140.000	22.523	23.670	24.850
143.600	22.489	23.634	24.812
145.000	22.438	23.580	24.756
150.000	22.376	23.515	24.688
155.000	22.366	23.505	24.677
160.000	22.335	23.472	24.643
161.600	22.332	23.469	24.639

\* cal deg.<sup>-1</sup> mole<sup>-1</sup>

TABLE 5

EXPERIMENTAL ENTROPY OF ADSORBED STATE ( $S_G' - (S_G' - \bar{S}_s)$ )  
 $\bar{S}_s$  (cal. deg<sup>-1</sup> mol<sup>-1</sup>)

Coverage	<u>Tetrachloroethylene</u>		<u>Trichlorofluoromethane</u>	
	Adsorption	Desorption	Adsorption	Desorption
5.0	67.22		57.07	
0.0	65.65		55.60	
15.0	64.88		47.04	
20.0	64.56		53.96	
22.1	64.39		-	
25.0	67.27		53.43	
30.0	63.84		53.09	
35.0	63.66		-	
40.0	63.16		52.87	
44.1	62.55		-	
50.0	61.51	62.28	52.27	
60.0	60.29	61.10	52.26	48.60
66.2	59.87	60.45	-	
70.0	59.57	60.12	-	50.43
75.0	59.19	59.35	52.32	50.81
80.0	59.05	59.4	52.37	51.02
85.0	58.79	59.23	52.42	51.40
88.2	58.61	-	-	-
90.0	88.56	59.15	-	-
100.0	58.36	58.47	52.42	51.21
105.0	58.39	58.86	52.46	51.30
110.0	58.25	58.8	-	

TABLE 5 (CONT'D)

Coverage	<u>Tetrachloroethylene</u>		<u>Trichlorofluoromethane</u>	
	Adsorption	Desorption	Adsorption	Desorption
115.0	58.26	59.34	52.43	51.59
120.0	58.25	58.90	52.43	51.76
125.0	58.32	58.99	-	-
130.0	58.15	58.9	52.61	51.89
132.3	58.12	-	-	-
140.0	57.94	58.70	52.38	51.90
145.0	57.89	58.68	-	-
150.0	57.74	-	52.32	52.19
154.4	57.71	58.02	-	-
160.0	57.68	58.52	52.30	52.09
165.0	57.68	-	-	-
170.0	57.66	58.38	52.22	-
176.4	57.63	58.59	-	-
180.0	57.64	58.64	-	-
185.0	57.62	58.66	52.25	-
190.0	57.52	58.64	52.22	-
198.5	57.59	58.63	-	-
205.0	57.59	58.61	-	-
210.0	57.58	58.56	-	-

THEORETICAL ENTROPY CHANGES ( $s_G^O - \bar{s}_S$ ) FROM THREE DIMENSIONAL TO TWO DIMENSIONAL GAS,  
ENTROPIES OF TWO DIMENSIONAL GAS FOR TETRACHLOROETHYLENE AND TRICHLOROFLUOROMETHANE AT 20°C.

$\theta^\dagger$	Coverage ( $\mu$ moles)	<u>Tetrachloroethylene</u>		<u>Trichlorofluoromethane</u>		
		$s_G^O - \bar{s}_S^*$	$\bar{s}_S^*$	Coverage	$s_G^O - \bar{s}_S^*$	$\bar{s}_S^*$
.1	4.41	26.93	55.21	3.59	17.88	54.55
.2	8.82	28.90	53.23	7.18	19.76	52.67
.3	13.23	29.28	52.85	10.77	20.15	52.28
.4	17.64	31.68	50.45	14.36	22.54	49.89
.5	22.05	33.14	48.99	17.85	23.90	48.53
.6	26.46	34.94	47.19	21.54	25.80	46.63
.7	30.87	37.48	44.65	25.13	28.34	44.09
.8	35.28	41.85	40.28	28.72	32.72	39.71
.9	39.69	53.40	28.73	32.31	44.26	28.17

\* cal deg<sup>-1</sup> mole<sup>-1</sup>

† number of monolayers

TABLE OF  $\theta$  AND  $\frac{-1}{\log P/p_0}$  FOR  
INVERSE KELVIN EQUATION PLOT

Tetrachloroethylene

<u>Adsorption</u>				<u>Desorption</u>			
$\theta$	20°	5.8°	-7.45°	$\theta$	20°	5.8°	-7.45°
0.113	0.637	0.650	0.669	0.17	-	-	0.769
0.227	0.804	0.814	0.852	0.227	-	-	0.794
0.340	0.947	0.965	1.017	0.340	-	-	0.857
0.454	1.082	1.112	1.059	0.385	-	1.001	-
0.501	1.146	1.175	1.261	0.454	-	1.043	0.893
0.567	1.231	1.269	1.374	0.476	1.107	-	-
0.680	1.400	1.448	1.587	0.576	1.171	1.082	0.925
0.794	1.590	1.685	1.848	0.680	1.214	1.133	0.991
0.907	1.819	1.944	2.158	0.794	1.239	1.214	1.116
1.000	2.043	2.199	2.439	0.907	1.274	1.347	1.256
1.134	2.419	2.583	2.868	1.020	1.347	1.503	1.400
1.247	2.774	2.851	3.256	1.152	1.512	1.724	1.581
1.361	3.128	3.303	3.627	1.247	1.661	1.881	1.724
1.501	3.627	3.794	4.228	1.361	1.855	2.037	1.902
1.587	3.947	4.122	4.566	1.474	2.071	2.310	2.094
1.701	4.350	4.537	5.018	1.587	2.310	2.520	2.322
1.814	4.753	4.933	5.461	1.728	2.647	2.805	2.589
1.927	-	5.214	5.838	1.814	2.805	2.999	2.774

$\theta$	$20^\circ$	$5.8^\circ$	$-7.45^\circ$	$\theta$	$20^\circ$	$5.8^\circ$	$-7.45^\circ$
2.000	5.364	5.522	6.086	1.927	3.067	2.237	3.008
2.041	5.501	5.666	6.207	2.041	3.322	3.724	3.265
2.268	6.278	6.378	7.097	2.154	3.617	3.748B	3.552
2.381	6.614	6.752	7.582	2.304	4.008	4.122	3.899
2.501	7.009	7.158	8.039	2.381	4.212	4.309	4.108
2.608	7.348	7.547	8.511	2.494	4.492	4.598	4.392
2.721	7.716	7.930	8.985	2.608	4.753	4.933	4.706
2.835	8.006	8.313	9.560	2.721	5.018	5.269	5.000
2.948	8.432	8.811	9.980	2.880	5.423	5.793	5.461
3.000	8.638	9.033	10.204	2.948	5.624	6.017	5.602
3.175	9.363	9.766	10.741	3.061	5.903	6.406	5.814
3.288	9.814	10.267	11.186	3.175	6.207	6.723	6.231
3.401	10.267	10.762	11.601	3.288	6.532	7.008	6.481
3.500	10.616	10.989	11.976	3.456	7.037	7.413	7.221
3.742	11.389	11.751	12.853	3.741	7.681	8.006	7.752
3.855	11.820	12.121	13.298	3.855	8.347	8.271	8.117
4.000	12.277	12.771	13.774	4.032	5.554	8.636	8.636
4.082	12.483	13.021	14.065	4.082	8.681	8.726	8.857
4.195	12.853	13.298	14.493	4.195	8.945	8.945	9.174
4.308	13.210	13.774	14.925	4.308	9.217	9.173	9.416
4.500	13.672	14.378	15.873	4.422	9.515	9.938	9.718
4.648	14.164	14.815	16.666	4.535	9.823	9.662	10.040
4.762	14.599	15.038	17.241	4.608	10.040	9.871	10.204

APPENDIX 11 (CONT'D)

$\theta$	$20^{\circ}$	$5.8^{\circ}$	$-7.45^{\circ}$	$\theta$	$20^{\circ}$	$5.8^{\circ}$	$-7.45^{\circ}$
4.875	14.925	15.385		4.762	10.373	10.267	10.672
5.000	15.267	15.873		4.875	10.672	10.493	10.989
				4.989	10.929	10.799	11.325
				5.184	11.390	11.325	11.820
				5.215	11.521	11.392	11.891
				5.329	11.820	11.669	12.195
				5.442	12.121	12.048	12.610
				5.555	12.438	12.285	12.853
				5.669	12.686	12.690	13.123
				5.760	12.936	12.937	13.477

TABLE OF  $\theta$  AND  $\frac{-1}{\log P/p_0}$  FOR  
INVERSE KELVIN EQUATION PLOT

Trichlorofluoromethane

<u>Adsorption</u>				<u>Desorption</u>			
$\theta$	20°	5.8°	-7.45°	$\theta$	-7.45°	5.8°	20°
0.139	0.596	0.581	0.519	1.393	1.999	2.373	2.762
0.279	0.737	0.721	6.704	1.501	2.077	2.459	2.820
0.418	0.884	0.937	0.833	1.532	2.111	2.472	2.828
0.501	0.974	0.943	0.903	1.071	2.236	2.554	2.999
0.557	1.035	1.004	0.965	1.811	2.399	2.676	3.024
0.696	1.218	1.175	1.116	1.950	2.597	2.860	3.228
0.836	1.431	1.378	1.304	2.000	2.684	2.948	3.312
1.000	1.734	1.676	1.618	2.089	2.851	3.155	3.490
1.114	2.010	1.944	1.834	2.228	3.147	3.563	3.828
1.253	2.486	2.367	2.230	2.368	3.470	3.935	4.254
1.393	2.990	2.851	2.698	2.501	3.828	4.254	4.721
1.501	3.400	3.228	3.058	2.646	4.188	4.613	5.195
1.671	4.48	3.864	3.659	2.786	4.537	4.968	5.666
1.811	4.785	4.450	4.188	2.925	4.866	5.325	6.064
1.956	5.423	5.071	4.817	3.000	5.053	5.522	6.277
2.000	5.685	5.288	5.001	3.203	5.624	6.135	6.863
2.089	6.086	5.666	5.441	3.343	5.995	-	7.220
2.228	6.725	6.254	6.017	3.482	6.402	7.037	7.610
2.368	7.353	6.835	6.614	3.501	6.456	7.128	7.680
2.501	7.893	6.916	7.158	3.621	6.780	7.547	8.039

<u>Trichlorofluoromethane</u>							
$\theta$	$20^{\circ}$	$5.8^{\circ}$	$-7.45^{\circ}$	$\theta$	$-7.45^{\circ}$	$5.8^{\circ}$	$20^{\circ}$
2.646	8.511	8.006	7.752	3.760	7.189	8.078	8.475
2.786	9.124	8.598	8.271	3.900	7.610	8.598	8.945
2.925	9.662	9.174	8.857	4.000	7.893	8.897	9.268
3.000	9.980	9.416	9.033	4.039	8.039	9.124	9.363
3.203	10.799	10.267	9.872	4.178	8.475	9.615	9.823
3.343	11.390	10.799	10.320	4.318	8.897	10.000	10.373
3.501	12.121	11.389	10.928	4.457	9.320	10.493	10.870
3.621	12.195	11.820	11.820	4.501	9.461	10.616	11.062
3.760	13.210	12.438	11.976	4.596	9.737	10.870	11.390
3.900	13.870	12.937	12.516	4.735	10.204	11.325	12.422
4.000	14.367	13.387	13.021	4.875	10.616	11.669	12.438
4.178	15.267	14.065	13.569	5.000	11.062	12.121	12.937
4.318	15.870	14.493	14.065	5.153	11.468	12.516	
4.457	16.667	-	-	5.292	11.891	12.833	
4.501	16.807	15.038	14.921	5.571	12.771	13.477	
4.596	17.241	-	-				
4.735	18.018	16.129	15.625				
4.875	18.832	16.667	16.129				
5.000	19.048	17.094	16.667				
5.153	20.162	17.699	17.391				
5.292	20.964	18.182	17.857				
5.571	21.834	19.194	19.011				

ADDENDUM 1

EXAMINERS' COMMENTS AND REPLIES TO THESE

I. Comments by Professor D.H.Davies

1. This project appears to be a part of a larger study of active salts, and yet no mention of these compounds or of the overall study is made. Standing alone, the thesis does not seem to have any point, and I feel that some attempt should have been made either in the introduction or in the discussion to show why the work was undertaken.
2. No information is presented to prove that the sample of nickel sulphate employed is actually the anhydride. At the temperature of preparation ( $120^{\circ}\text{C}$ ), I should have expected the active monohydrate to be produced. Further work is required to establish the nature of the absorbent. Studies of the weight loss during preparation and of the heat of solution after preparation would be informative.
3. Equation 20 is correct. However, it would be desirable to specify that a cylindrical meniscus for which the mean radius of curvature is twice the radius of the cylinder is being considered. Nevertheless, I do not agree with the substitution of  $r = \delta(\theta - X)$  nor do I think that the use of the Kelvin equation to calculate the contact angle is justified since its applicability to capillaries of these dimensions is uncertain.
4. The shape of hysteresis loop observed could have

been produced by open slit-shaped capillaries with parallel walls as postulated, or by very wide capillaries with narrow openings. Are there any structural data available which would allow a choice to be made?

5. It is contended that the upper closure point of the hysteresis loop is asymptotic with the saturation vapour pressure and that 'it was necessary to adsorb a large excess of adsorbate in order to obtain a .... reproducible ....desorption curve'. No data are presented to establish the former statement, and it is difficult to understand the meaning of "a large excess" in the latter. As the candidate has pointed out, unless the experiments are extended to the saturation vapour pressure, the desorption points will lie on scanning curves which are meaningless if the descending boundary curve is unknown. It appears that no attempts were made to reach saturation, and that with the sample weight employed it would have been impossible to measure the saturation adsorption. A smaller weight of sample ought to be employed so that the important saturation region of the isotherm can be investigated.
6. If the upper closure point were observed to be asymptotic with the saturation vapour pressure, an observation which would be difficult if not impossible with the present experimental system, it could be caused, for example, by radiation heat transfer. In order to obtain reproducible saturation values, it is often necessary to protect the sample from radiation with a silvered jacket (see for example, Hooley, Can.J.Chem.1962, 40,745).

As Quinn et al (Can.J.Chem.1955,33,286) did not seem to have any difficulties with the active monohydrates of several salts, I cannot believe that such an observation is characteristic of the sample.

7. Open, slit-shaped capillaries with parallel walls will fill with adsorbent when the thickness of the adsorbed layer is one half the distance between the walls. If the pores are to contribute to the hysteresis phenomenon, this will only occur near saturation. On desorption, a cylindrical meniscus will be formed provided there is sufficient adsorbed material to produce liquid-like properties. Under these conditions, the mean radius of curvature of the cylindrical meniscus will be  $(r-2t)$  where  $r$  is the separation of the walls and  $t$  is the thickness of the adsorbed layer at the relative pressure at which the pore empties. It is difficult to estimate  $t$ , but I would expect it to be at least  $5 \text{ \AA}$ . Therefore the estimated spacing of  $12 \text{ \AA}$  is much too low and I would suggest a spacing of perhaps  $20-25 \text{ \AA}$ . In any case, the relative pressure at which the loop closes is usually more characteristic of the adsorbate than of the adsorbent, and therefore a radius calculated from this value may have no significance for the adsorbent except to show that pores of this dimension are present.

## II. Reply to Comments of Professor D.H.Davies.

1. The work grew only incidentally from the study of adsorption on inorganic salts. The purpose of this work was to elucidate the nature of the sorption hysteresis occurring

with anhydrous nickel sulfate. In addition, the purpose was to test the use of the Kelvin equation in the study of capillary condensation.

2. The weight lost by the sample indicates that the salt was in the anhydrous form.

3. The thesis investigates the applicability of the Kelvin equation to condensation in small capillaries. The thesis finds (Figures 16,17 and 18) that the Kelvin equation does seem to apply. While the precise nature of the contact angle may be debated, the equation indicates that this angle must be considered to have a finite value in the case studied, and is not zero as is usually assumed.

The assumption that the contact angles are zero where capillary condensation occurs is usually made on the basis that exact knowledge of the contact angles is now available. The information in this thesis, that contact angles are finite has certainly a more sound basis.

4. Large capillaries with narrow openings would produce a hysteresis curve of type E. Reference to the structure of anhydrous nickel sulfate is given in reference 40 in the thesis.

5. Upper regions of the isotherms were asymptotic with saturation vapour pressure. The desorption loops, as is obvious from the data shown in Appendix 4, were reproducible over the lower portion of the branches as is stated in the thesis.

A smaller sample would mean a smaller amount adsorbed at lower pressures. Since the focus of interest was upon these lower regions, a smaller sample weight was considered undesirable.

6. The system studied by Hooley (Hooley, Can.J.Chem. 1962, 40,745), studied light sensitive adsorbents which formed complexes with the adsorbate. The relevance to the present system is not obvious.

Quin et al (Can.J.Chem.1955,33,286) studied the adsorption of argon on monohydrates and give no data for the desorption isotherm on  $\text{NiSO}_4 \cdot \text{H}_2\text{O}$ . Again, the relevance is not obvious.

7. The pores between parallel plates will contribute to hysteresis when

- a. The adsorbed layers are thick enough to bridge the gap between plates.
- and b. b. The adsorbed layers exhibit liquid like properties.

As is shown in the thesis, saturation vapour pressure is not a necessary criterion.

The value of  $t$  was estimated in terms of the appearance of liquid like behaviour according to the Kelvin equation.

### III. Comments of Professor D. Barton

1. The introduction is extremely brief and is not of much help to a non-specialist. Various postulates and theories are mentioned and references are given but not much is said about them.

2. This paragraph (all of page 11) is not properly part of the introduction and should be deleted. The context, which is a summary of the work to be presented, is covered in both the abstract and the summary.

3. The statistical thermodynamics of adsorption is evidently an extremely complicated problem. While I have no objection to the inclusion of the two dimensional gas model, I think that the limitations and status of the model should be discussed. The one sentence introduction to this section is not sufficient. On page 49 it is suggested that the difference between calculated and measured entropy for tetrachloroethylene may be due to a weak vibration, however no mention is made of the same possibility for trichlorofluoromethane, for which the measured and calculated entropies more nearly coincide. Also no mention is made of how much entropy would be contributed by a weak vibration, or of any other reasons for the lack of fitting.

Reply to Comments of Professor D. Barton.

1. The thesis assumes some knowledge of surface chemistry although no expertise in the field, on the part of the reader is required.

2. The content of the introduction was determined partly in terms of the practice here. The portion on page 11 enlarges upon the abstract and gives direction to the readers' thoughts as he enters the main body of the thesis.

3. To elaborate the two dimensional gas model would be irrelevant. The model is introduced only as a possible form of the adsorbate over a short range of relative pressures. The range of pressures on which the study concentrates is above that at which the two dimensional model applies.

Regarding the magnitude of the vibrational contribution - assignment of a particular value is, unfortunately, arbitrary. Any assignment would, as far as elucidating the state of the adsorbent, be illusory.





